Geochemistry of fluids discharged over the seismic area of the Southern Apennines (Calabria region, Southern Italy): implications for Fluid-Fault relationships

Italiano F. [(1)], Bonfanti P. [(1)], Pizzino L. [(2)], Quattrocchi F. [(2)]

(1) INGV, Sezione di Palermo, via U. La Malfa 153, Palermo (Italy)

(2) INGV, Sezione di Roma 1, via di Vigna Murata, Roma (Italy)

Abstract

The first comprehensive geochemical data-set of the fluids circulating over a 14,000 km^2-wide seismic-prone area of the Southern Apennines, Calabria Region (Italy), is presented here. The geochemical investigations were carried out with the twofold aim of constraining the origin and interactions of the circulating fluids and to investigate possible relationships with the local faults. We collected 60 samples of both thermal and cold waters which the dissolved gases were extracted from. The geochemical features of the water samples display different types and degrees of water-rock interactions, irrespective of the outlet temperature. The calculated equilibrium temperatures of the thermal waters (60-160°C) and the low heat flow of the whole study area, are consistent with a heating process due to water deepening and a fast upraise through litospheric structures. The composition of the dissolved gases reveals that crustal-originating gases (N_2 and CO_2-dominated) feed all the groundwaters. The $^3He/^4He$ ratios of the dissolved helium, in the range of 0.03 to 0.22Ra_c for the thermal waters and 0.05-0.63Ra_c for the cold waters (Ra_c = helium isotope ratio corrected for atmospheric contamination), are mainly the result of a two-component (radiogenic and atmospheric) mixing, although clues of mantle-derived helium are found in some cold waters. As the study area had been hit by 18 of the most destructive earthquakes (magnitude ranging from 5.9 to 7.2) occurring over a 280-year time span (1626-1908) in Southern Apennines, the reported results on the circulating fluids may represent the reference for a better inside knowledge of the fault-fluid

relationships and for the development of a long-term geochemical monitoring of the area.

Key Words: Dissolved gases, helium and carbon isotopes, tectonic structures, Southern Apennines, Calabria Region (Italy).

1 - Introduction

This paper accounts for the first results gained by some geochemical surveys carried out over one of the most seriously seismic-prone areas of the Apennine chain. This area, located at the southernmost part of the Italian peninsula (Calabria Region), was repeatedly razed to the ground (18 times from 1626 to 1908; Boschi et al., 2000) by 5.9 <M< 7.2 destructive events (Gruppo di Lavoro CPTI, 2004; Fig. 1). After the destructive 1908 Earthquake (some 100,000 victims, 90% of the buildings destroyed in the cities of Messina and Reggio Calabria), the area's on-shore seismicity has been very low with M > 4, about 200 shocks with 3 < M < 4 (Fig. 2) out of a total of 3,800 events occurring between 1980 and 2005 (Castello et al., 2006; Gruppo di Lavoro CPTI, 2004). The recorded seismicity is marked by focal depths less than 30 km (i.e. crustal). Considering this kind of seismic gap, the chance to record modifications in the fluids due to severe developments of the seismogenetic processes is an attractive scientific perspective for this area, thus broadening interest in the proposed results.

In fact, it is well-known how changes in fluid composition and behaviour occurs over any seismic area (see Thomas, 1988; Martinelli, 1997; Toutain and Baubron, 1999). As the whole hydrological circuit depends on rock permeability, the geochemical features are also sensitive to permeability changes occurring, for example, as a consequence of faulting activity (e.g. King, 1986; Thomas, 1988; Toutain and Boubron, 1999; Italiano et al. 2001, 2007; Caracausi et al. 2005).

Although the investigated area of the Calabria region is renowned for a variety of thermal waters known about since Roman times, knowledge of the circulating fluids is very poor and only very little geochemical information is available today. In this paper we focus our attention on the thermal and

cold waters, including the dissolved gas phase, with the aim of defining its geochemical features and providing an initial comprehensive geochemical data set.

During field surveys carried out between 1993 and 2007, sixty samples were collected from a total of 44 different sites: 30 of them are thermal waters and 30 cold waters from springs and wells. Following the NOAA (National Oceanic and Atmospheric Administration) Geophysical Data Centre indications, we considered a temperature of 20°C at the emission point as the boundary limit between the two groups (thermal waters $T \geq 20$°C; cold waters $T < 20$°C). The results obtained have allowed us to gain an insight into the nature of the circulating fluids and to discover the role of some local faults in determining their geochemical features.

2 - Geotectonic outlines and seismicity

The investigated area represents the southern segment of the Apennine Chain known as the Calabrian Arc (hereafter referred to CA); it is a well-developed, arc-shaped structure of the circum-Mediterranean orogenic belt. It represents an accretionary wedge, caused by the Africa–Europe collision (Amodio-Morelli et al., 1976; Tortorici, 1981), consisting of a series of ophiolite-bearing tectonic units (Liguride Complex; Ogniben, 1969), and overlying basement nappes (Calabride Complex; Ogniben, 1969), as shown in Fig. 2 There is general agreement in the literature on the geometrical position of the different units, and their ages: from bottom to top, Mesozoic carbonates, Mesozoic ophiolites, Paleozoic-Mesozoic slates and metapelites, Paleozoic orthogneisses, and Paleozoic paragneisses.

Since Middle Miocene, over-thrusting, combined with the progressive south-eastwards migration of the CA along a NW-SE to WNW-ESE-trending regional strike-slip fault system (Ghisetti and Vezzani, 1981; Tansi et al., 2005; Tansi et al., 2007) was associated with the opening of the Tyrrhenian basin (Amodio-Morelli et al., 1976; Ghisetti and Vezzani, 1982). These conditions imply the existence of a kinematic de-coupling in the Northern sector of the Calabrian Arc, which allows for differential movement relating to the Southern Apennine Chain. This decoupling

structure is traditionally identified, on the surface, with the strike-slip "Pollino" Fault, bordering the slopes of the Pollino Chain, active from the Tortonian to the Pliocene age (Van Dijk et al., 1995). In the Neotectonic Map of Italy (Ambrosetti et al., 1987) a quaternary activity has been associated to this fault. The whole system consisted of Middle Miocene-Middle Pleistocene crustal oblique transpressional fault zones, mainly dipping toward NE and characterized by left-reverse movements, along which the extrusion of the deep-seated units of the CA together with underlying Mesozoic carbonate rocks occurred. Large Mesozoic carbonate bodies outcrop in northern Calabria, while a few others are exposed throughout the Region, such as along the Catanzaro line (Fig. 1). In the literature, they are traditionally considered as "tectonic windows" of the Apennine Chain (e.g. Amodio-Morelli et al., 1976; Tansi et al., 2007; Tortorici, 1981). Since the Middle Pleistocene, an intense WNW-ESE oriented regional extensional phase occurred, resulting in a ≈ 370 km-long fault belt consisting of a 10 to 50 km-long distinct normal fault segment running along the western side of the CA, both offshore and on land (Catalano et al., 2008). These normal faults, trending N-S to NE-SW (Tansi et al., 2005), are also responsible for the region's crustal seismicity; both geological and morphological observations indicate that these normal active faults are characterized by throw-rates ranging from 0.5 to 3.1 mm/a (Jenny et al., 2006; Catalano et al., 2008). The development of the rift-zone was coupled with a strong regional uplifting of the whole CA; this process is still active (Dumas et al., 2005). It probably represents the response to the isostatic rebound due to detachment of the Ionian subducted slab (Westaway, 1993; Tortorici et al., 1995; Tortorici et al., 2003). The most evident consequence of the widespread Quaternary uplift process is the occurrence of a spectacular flight of marine terraces, developed mainly along the Tyrrhenian coastline of Calabria, as a result of the interaction between the tectonic uplift and Quaternary cyclic sea-level changes (Bosi et al., 1996). According to Ghisetti and Vezzani (1982), during the Late Pliocene-Early Quaternary, the CA was dissected by longitudinal and transversal normal faults; these faults caused the fragmentation of the arc into structural highs and marine sedimentary basins (e.g. Crati valley, the Gioia Tauro plain and the Crotone basin, Fig. 1).

In a recent paper, Basili et al. (2008) describe the evolution in mapping and archiving Italian active fault data in relation to important achievements in the understanding of Italian tectonics in the last 20 years. In Fig. 1 we report the main active faults of the Calabria region (Valensise and Pantosti, 2001; Basili et al., 2008), as well as the location of the most catastrophic earthquakes that struck Calabria between 1626 and 1908 (18 events with M ranging from 5.9 to 7.2, as reported in the *Catalogo Parametrico dei Terremoti Italiani* (Gruppo di lavoro CPTI, 2004). Most events occurred in clusters, spanning several months to years. The most remarkable earthquakes, with M ≥ 5.9, took place (Fig. 1): i) in northern Calabria in 1836, with M = 6.2; *ii*) in the Crati valley in the time interval 1835-1870 (three earthquakes with M ranging from 6.0 to 6.2 occurred in 1835, 1854 and 1870); *iii*) in central Calabria (Crotone basin) in 1638 and 1832, with M 6.5 and 6.6, respectively; *iv*) in central-southern Calabria in 1626, 1638, 1659, 1791 and 1905 with M ranging from 5.9 to 7.1. The most ruinous seismic sequence that struck the Calabria region occurred in the Gioia Tauro plain and in the Catanzaro trough in 1783, consisting of five events, the largest having magnitudes of about 7, and *v*) in southern Calabria in the period 1894-1908, with M comprised between 5.9 and 7.2. In central and southern Calabria, all major earthquakes have been related to primary N-S and NE–SW trending normal faults (Tansi et al., 2005, 2007; Jenny et al., 2006; Mattei et al., 2007); fault-plane solutions of crustal earthquakes (mainly micro and moderate earthquakes) recorded in recent years, have highlighted the extensional or strike-slip character of the present shallow tectonics (Moretti and Guerra, 1997; Tansi et al., 2005). Beneath the crust, compressive focal mechanisms have been found, possibly correlated to the ongoing flexing of the ionic plate. Since 1908, Calabria has been seismically quiet, at least for M>4 (Gruppo di Lavoro CPTI, 2004; Castello et al., 2006).

3 - Sampling and analytical procedures

This paper accounts for the thermal and cold waters collected over the Southern Apennine, between 37°54' and 39°54' latitude N. All the water samples were considered for chemical and isotopic analyses as well as for the extraction and analysis of the dissolved gases.

Samples were collected at 44 different sites including spas, wells and springs (see column 6 in Table 1 and Figure 1 for their geographical location;), during geochemical surveys carried out in the Calabria region over a time range of more than 10 years (1993, 1994, 1995, 2000, 2001 and 2007). We sampled 30 thermal waters (outlet temperatures ranging between 21.8 and 43.6°C), and 30 cold waters showing outlet temperature ranging between 10 and 21.4°C). Although sampling procedures and analytical methodologies have changed over time, the collected results are wholly comparable.

3.1 –Waters

The analytical determinations included field measurements (T°C, pH, Eh, electrical conductivity and alkalinity) and laboratory analysis. pH, Eh and conductivity were measured by electronic instruments calibrated *in situ* using buffer solutions. The temperature was measured by both mercury and (recently) digital thermometers having resolution of 0.01°C and error of ± 10%. Samples were collected in triplicate and stored as "as is sample", filtered sample (0.45 μm filter) and "filtered and acidified" (HNO_3 suprapur-grade acid). In the laboratory, the chemical composition was determined by liquid chromatography (Dionex 2001) using a Dionex CS-12 and a Dionex AS4A-SC column for cations and anions determinations, respectively. The HCO_3 content (i.e. alkalinity) was measured by standard titration procedures with hydrochloric acid.

Isotope determinations (D/H and $^{18}O/^{16}O$) on water samples were performed by the equilibration technique (Epstein and Mayeda, 1953 for oxygen) and water reduction (hydrogen production by using granular Zn, Kendall and Coplen, 1985), respectively. Measurements were carried out using a Finnigan Delta Plus mass spectrometer (Hydrogen) and an automatic preparation system coupled with an AP 2003 IRMS (Oxygen). Analytical precision for each measurement is better than 0.2‰ for $\delta^{18}O$ and 1 ‰ for δD.

3.2 - Dissolved gases

The dissolved gases were extracted from water following two different procedures: the gas phase dissolved in samples collected in 1993-1995 was extracted in the laboratory from a 500ml water sample in a vacuum line. The dissolved gases from samples collected in 2001 and 2007 had been extracted following the equilibration method (Capasso and Inguaggiato, 1998) from water samples stored in 240ml glass bottles that were sealed in the field by silicon/rubber septa using special pliers. All the samples were collected taking care to avoid even tiny bubbles so as prevent atmospheric contamination. Chemical analyses were carried out by quadrupole mass spectrometry on those samples extracted in the vacuum line, while the gas phase extracted after the attainment of the equilibrium with the, high-purity argon host-gas (see Sugisaki and Taki, 1987 and Capasso and Inguaggiato, 1998 for details) were analyzed by a gas-chromatograph (Perkin Elmer 8500) equipped with a double detector (TCD-FID) using argon as carrier gas.

Helium isotope analyses were carried out only on samples collected in 2001, 2003 and 2007. The gas fractions extracted following the same procedure as for the gas-chromatography were purified following methods already put forward (e.g. Sano and Wakita, 1988, Hilton 1996, Italiano et al 2001). The isotopic analyses of the purified helium fraction were performed by a static vacuum mass spectrometer (GVI5400TFT) that allows for the simultaneous detection of ^{3}He and ^{4}He-ion beams, thereby keeping the $^{3}He/^{4}He$ error of measurement to very low values. Typical uncertainties in the range of low-3He (radiogenic) samples are within ± 5%.

The method for the determination of $\delta^{13}C_{TDIC}$ is based on chemical and physical CO_2 stripping. The stripped gas is purified by means of standard procedures. The isotopic values were measured using a Finnigan Delta Plus mass spectrometer and the results are reported in δ ‰ vs. V-PDB standard. The standard deviation of the $^{13}C/^{12}C$ ratio is ± 0.2 ‰.

4 - Results

The location of the study sites is listed in Table 1 and given in UTM-WGS84 coordinates. Fig. 1 displays the distribution of the sampling sites in the frame of the local heat flow setting (Cataldi et al., 1995), besides the seismogenic faults (Valensise and Pantosti, 2001; Basili et al., 2008) and the epicentral location of the main historical earthquakes (Gruppo di lavoro CPTI, 2004).

The chemical and isotopic composition of the water samples is reported in Table 2 (2a thermal waters; 2b cold waters), while the chemical features of the dissolved gases are listed in Table 4 (a and b). Isotopic compositions of carbon (TDIC) and helium are reported in Tables 5 and 6, respectively. To enhance the differences in their geochemical features, the analytical results of both thermal and cold waters are graphically presented together.

4.1 – Thermal and cold waters

Thermal waters show outlet temperatures ranging between 21.8 and 43.6°C, salinity (expressed as Total Dissolved Solids or TDS) between 0.8 and 10 g/l, pH between 6.42 and 9.01 and Eh between -366 and 289 mV. Cold waters show outlet temperatures ranging between 10.1 and 21.4°C, salinity (expressed as TDS) between 0.1 and 22 g/l, pH between 6.29 and 8.20 and Eh between -322 and 387 mV. Such a large variability in the physical-chemical parameters measured both in thermal and cold waters is driven by different geochemical processes (i.e. water-rock interaction, mixing between aquifers, dissolution of gases of different origins, repeated gas-water interactions, etc.) occurring during the hydrological paths, which affect the final water's characteristics. Considering those processes, we describe the chemical composition of the water samples, in terms of: *i*) major ion contents, in the Langelier-Ludwig diagram of Fig. 3; *ii*) Ca, Mg and Na+K contents (triangular plot of Fig. 4a) and *iii*) Cl, SO_4 and HCO_3 contents (triangular plot in Fig. 4b). The reported diagrams indicate the occurrence of the following waters types:

Ca-HCO_3 (samples 34, 36-38, 42 and 48-50 and 54-60). Cold waters discharging in the central-northern sector of the Gioia Tauro Plain as well as in the Sila and Aspromonte Massifs. Both chemical and physical characteristics suggest that they migrated through shallow hydrological

circuits, characterized by limited interactions with local rocks (including soils). Three samples of the Aspromonte massif (51, 52 and 53), facing the Tyrrhenian sea, evolve towards a Na-Cl chemistry (Fig. 3) due to the marine spray contamination, predominant over the limited water-rock interaction process. The bulk of the waters discharging in the Gioia Tauro Plain has a distinctive sulphurous smell and are locally known as "sulphurous waters"; they are marked by negative Eh values suggesting their circulation in reducing environments.

Na-HCO_3 (samples 39, 40 and 47). Cold waters discharging in the Gioia Tauro Plain. These waters belong to a circuit flowing in a sandy aquifer; they interact and equilibrate with clayey strata forming the top and the bottom of the aquifer itself. As testified by the artesian discharges, this aquifer is in hydrostatic equilibrium. The samples represent typical alkaline waters, probably owing to the peculiar chemical composition of cation exchange processes, leading to a generally strong decrease in the Ca and Mg content (adsorbed by clays) and a contemporaneous Na-enrichment (released by clays) of the solution (Figs 3 and 4a).

Ca-SO_4 waters (samples 3-7, 27-28, 31, 33, 35, 41, 43-44). Cold and thermal waters. The former discharge over the Sibari Plain, the Crati Valley and the Crotone basin, while the latter discharge at the foot of the Pollino massif and in the Catanzaro trough (Caronte spa, samples 3-4). The calcium-sulphate chemistry of these waters (sometimes enriched in Mg, Fig. 4a) could generally be attributed to the leaching of evaporite formations (mainly consisting of gypsum) contained: *i*) in the shallowest layers (Messinian age) of the Crati valley and Crotone basin; *ii*) at the bottom of the Mesozoic carbonate formation (Trias age) in northern Calabria and *iii*) in the Mesozoic carbonate and dolomite rocks out-cropping within a tectonic window in the Catanzaro trough. The different depths reached by the hydraulic circuits (deeper for the thermal waters group, samples 3-7, 27-28- than the cold water group, samples 31, 33, 35, 41, 43-44) are strongly emphasized by the water temperatures measured at the discharging points.

Na-SO_4 waters (samples 8, 15, 16, 23, 24). These H_2S-rich samples are thermal waters representing the surface expression of the low-enthalpy geothermal systems of Galatro, hosted in the granites of

the Aspromonte Range (Gioia Tauro Plain), Cerenzia and Repole, hosted in the neogenic sediments of the Crotone basin. For the Galatro hot spring (samples 15 and 16) the observed chemistry could be explained by a shallow interaction of the uprising deep Na-Cl thermal waters with shallow clayey strata (uptake of Ca and Mg and Na-enrichment in solution) together with the shallow oxidation of H_2S to SO_4, determining the peculiar sulphate-enrichment (Fig. 4b). Cerenzia and Repole waters (samples 8 and 23 -24, respectively) deepen their circuits in the neogenic terrains of the Crotone basin and the observed chemistry could be the result of mixing between issuing Na-Cl waters and Ca-SO_4-bearing pore fluids; Ca removal due to shallow cationic exchange activity may be evoked, because of the huge and widespread presence in the area of marine clay outcrops.

Na (Ca)-Cl (SO_4) high salinity cold waters (samples 32, 45-46). These waters discharge into the northern sector of the Crotone Basin and show relatively high levels of SO_4, Ca and Mg (Figs 4a and b). Such geochemical features could be explained by leaching, to various extents, of halite-rich Messinian evaporites (strongly prolonged, in particular, for samples 45-46, having the same Na/Cl ratio and almost equal chemical composition than seawater, Fig. 3) contained in the neogenic formation of the basin.

Na (Ca)-Cl (SO_4) high-salinity thermal waters (samples 1-2, 9-14, 17-21, 25-26, 29-30). These waters discharge diffusely in the study area (southern Calabria, Crotone basin, Gioia Tauro Plain and northern Calabria (Sibari plain); they are located along regional fault systems (see Fig. 2) and represent the main issues of the low-enthalpy geothermal systems of Calabria (see later). Their chemical characteristics are affected by different geochemical processes, all enhanced by the intense faulting and fracturing, such as: *i*) significant mixing with seawater; *ii*) interaction with marine sediments and/or mixing with formation waters; *iii*) extensive and prolonged interaction with both metamorphic and igneous rocks. Locally, such as in the Gioia Tauro Plain, seawater is strongly involved both in the geothermal circuits and in water-rock interaction processes (Pizzino et al., 2004) as shown by the noteworthy Na enrichment (e.g. Rosarno thermal well, sample 25).

4.2. H and O isotopes

The $\delta D/\delta^{18}O$ diagram (Fig. 5) shows the distribution of the samples in respect to the "local" rainwater isotope composition (LMWL; Longinelli and Selmo, 2003) and the "mean" Mediterranean meteoric water line (MMWL Gat and Carmi, 1970). The slope of the $\delta D/\delta^{18}O$ waterline value provides information on the processes affecting the rainfall events; the value of 8 for the slope of the global Mediterranean water line suggests that the groundwaters are fed by precipitations occurring under near-isotopic equilibrium conditions. The discrepancy between "mean" and "local" rainwater isotope composition is a consequence of non-equilibrium processes, probably related either to the monthly amount of rainfall, or to the altitude and the relative humidity of the atmosphere. The evidence that almost all the samples, irrespective of their cold or thermal features, fall above the LMWL, highlights the importance of considering local references instead of generic indications (e.g. the MMLW). Both thermal and cold waters are slightly shifted with respect to the local meteoric line showing: *i*) a general deuterium excess that could be a consequence of fractionation processes due to H_2S exsolution (light isotope removal) from the water phase, with the typical sulphur smell of many sampled waters representing an evident clue of H_2S degassing and *ii*) a general decrease in the $^{18}O/^{16}O$ ratio probably due to the CO_2 loss during the ascent of circulating waters towards the surface. As a consequence, thermal waters do not show any isotopic shift in the oxygen (i.e. an increase in the $^{18}O/^{16}O$ ratio) due to water–rock exchange suggesting that, although the thermal waters interact with a large variety of host rocks, the water/rock interactions occur at a relatively low-temperature.

4.3. Geothermometric estimations

Chemical analyses of geothermal fluids may be useful in estimating subsurface reservoir temperatures in the geothermal systems. A number of geothermometric techniques have been proposed in the past decades (e.g. Fournier and Truesdell, 1973; Fournier, 1977; Fournier and Potter, 1979; Fouillac and Michard, 1981; Arnnorsson et al., 1983; Kharaka et al., 1985;

Giggenbach 1988; Kharaka e Mariner, 1989). The chemical geothermometers are based on the following theoretical assumptions: i) water and host rocks are in equilibrium as such water is saturated by the mineral phases governing the geothermometer; and ii) during the ascent towards the surface, the waters neither re-equilibrate nor mix with shallow circulating fluids.

The degree of water–rock equilibrium attained by geothermal waters in all the studied sites was evaluated by the Na–K–Mg triangular diagram first proposed by Giggenbach (1988) allowing for a distinction between suitable or unsuitable waters for the application of ionic solute geothermometers. Giggenbach (1988) divided thermal fluids into fully equilibrated, partially equilibrated, and immature waters as a function of their Na, K and Mg content(s). In accordance with this technique, we plotted our data on a modified version of the diagram (Giggenbach and Corrales, 1992) suitable for low-temperature geothermal systems (in the range of 20-220°C).

The Mg-Na-K triangular diagram (Figure 6) emphasises how almost all the collected thermal waters fall within the field of partially equilibrated waters, while the cold waters fall within the field of immature waters. Some exceptions are represented by the cold water samples from the Verzino (samples 45 and 46) and Casabona sites (sample 32), both located in the Crotone basin, and by the thermal water from Rosarno (sample 25). Samples from Verzino and Casabona sites issue in the eastern edge of the Strongoli-Cerenzia line and, probably, represent a mixing between thermal and cold water components. Rosarno well water, as claimed by Pizzino et al., 2004, is affected both by mixing with seawater and prolonged interaction with clays, causing significant Na enrichment; these processes minimise its utilisation in the deep temperature estimate by using Na geothermometers. Its position on the Mg-Na-K triangular diagram, out of the three fields indicated by Giggenbach, fully support our inferences.

The cold waters, mainly belonging to the immature waters group (Figure 6), show that they are not in equilibrium with the reservoir rocks and that the final chemical composition is probably dominated by several, contemporary active, processes such as rock dissolution, mixing with cold groundwaters and ion exchange making any calculated temperature equilibration unreliable. Table 3

lists the geo-temperatures obtained by the application of the specified gethermometers: the Na-K-Ca and Na-K geothermometers provide consistent results for almost all the thermal waters showing they come from aquifers with temperatures in the 140-160°C range, in agreement with the observation that no oxygen isotopic shift occurs during water/rock interactions. The calculated range of 41-98°C for the quartz geothermometer shows that a quartz loss occurs during uprising, mostly because of cooling processes. For some water groups (Antonimine, Cotronei, Gioia Tauro plain thermal wells) all the applied geothermometers provided comparable equilibration temperatures, denoting negligible cooling because of a fast uprise of the thermal waters, probably enhanced by local faults.

4.2 - Dissolved gases

The gas phase dissolved in groundwaters is considered a useful tool for understanding gas–water interactions in several environments of the shallow crust. The high mobility, coupled with the different solubility of the various gas species, makes gases excellent geochemical tools in tracing fluids in hydrological circuits. Although the results proposed here bring together data collected following different sampling and analytical procedures, the dissolved gas concentrations detected for 1993-1995 survey samples are comparable with those collected in 2001 and 2007 (Table 4, *a* and *b*).

Starting from the gas-chromatographic analyses, the composition of the dissolved gas phase (expressed as ccSTP; P=1bar; T=20°C) was calculated taking into account the solubility coefficients (Bunsen coefficient "β", cc_{gas}/ml_{water} STP) of each gas specie, the amount of gas extracted and the volume of the water sample. Then, considering the wide range of dissolved gas content, we recalculated the relative gas concentrations from cm^3 STP/l to volume % to make the analyses of the dissolved gases an homogeneous data set.

The analytical results show that the gases dissolved in the thermal waters are N_2-dominated (Tab. 4a) in contrast with the cold waters that bring a CO_2-dominated gas phase. The N_2-CO_2 binary

diagram of Figure 7 shows that for all the waters, independently from their salt contents, CO_2 and nitrogen together represent the majority (sometimes close to 100%) of the dissolved gas species. There are two different trends followed by the cold and thermal waters interpreted as the result of different water-gas interactions. Samples from the Cotronei site (9-14), for example, fall close to the X axis (above 90% of N_2 content) as CO_2 is almost totally lost. The residual gas phase is enriched in the less reactive, and also low soluble, gases (e.g. He content, Table 4a). This last evidence indicates that the dissolved gas composition is due to water-gas interaction processes (gas dissolution) instead of degassing. Contrastingly, the sample from the Cassano site (33b), displaying the highest CO_2 values besides the lowest N_2 content, highlights gas-water interactions to small extents. As a general remark, the variable proportions of He (Table 4, a-b) besides the N_2-CO_2 relationships (Fig. 7) are interpreted as a consequence of the gas dissolution processes, accounting for the high concentrations of total helium, in the $2.4x10^{-5} \div 3.6x10^{-3}$ cm^3 STP per litre range for the cold waters and $1.2x10^{-4} \div 5.9x10^{-2}$ cm^3 STP/l H_2O for the thermal waters. Thermal waters are more helium-concentrated than the cold waters by two orders of magnitude, supporting the hypothesis that the gas-water interaction processes proposed for the Cotronei sample is behaviour common to all the thermal waters. In all cases, He concentrations are in excess as compared with the air-equilibrated waters ($4.65x10^{-5}$ cm^3 STP/l H_2O at 20°C), consistent with the He influx coming from an external source. As a result of the limited gas-water interactions, the gas phase dissolved in the cold waters is probably representative of the CO_2-dominated gas phase typically degassed over the area.

4.5 Carbon isotopes

CO_2 undergoing gas-water interactions partially dissolves as bicarbonate ions, so the isotopic composition of the Total Dissolved Inorganic Carbon ($\delta^{13}C_{TDIC}$) is a useful geochemical tool for investigating gas-water interaction processes where CO_2 is the dominant gas specie. The primary natural CO_2-producers, such as mantle-derived products besides metamorphic and biogenic

contributions, have different isotopic signatures which, although partly overlapping and variable because of the isotope fractionation due to the CO_2 reactivity, may provide information on the original signature of the parent gas and the possible fractionation processes responsible for the final carbon isotopic composition.

Dissolved inorganic carbon is present in three chemical species in the groundwater: CO_2(aq), HCO_3^- and CO_3^{2-}. Gaseous CO_2 dissolves, and then isotopically equilibrates with CO_2(aq), as well as HCO_3^- and CO_3^{2-} in the aqueous phase. The mole fraction of each specie depends on the pH of the solution. In the pH range of the sampled waters (6.29-9.01, Tables 2 a, b) HCO_3^- is predominant, with minor CO_2(aq) and negligible CO_3^{2-}. As a consequence, the $\delta^{13}C_{TDIC}$ values depend mainly on the mole fraction of HCO_3^-. The TDIC, representing the sum of the dissolved inorganic carbonate species, was calculated using a dedicated software (*Phreeqc version 2.12*: Parkhurst & Appelo, 1999). As its isotopic composition represents the average of the isotopic composition of the dissolved carbon species (CO_{2aq}, HCO_3^- and CO_3^{2-}), the $\delta^{13}C_{TDIC}$ can be expressed as the isotopic balance of dissolved carbon species weighted on the respective inorganic carbon contents, and written (in a simplified form since all the samples have negligible CO_3 contents):

$$\delta^{13}C_{TDIC} = (\delta^{13}C_{CO2\,aq} * \chi CO_{2aq} + \delta^{13}C_{HCO3} * \chi HCO_3)/M \qquad (1)$$

where χ is the molar fraction and M is the total mass of dissolved carbon

The $\delta^{13}C_{CO2aq}$ and $\delta^{13}C_{HCO3}$ can be computed considering the isotope enrichment factors (ε) for CO_{2gas} - HCO_3 (ε_α) and CO_{2gas} - CO_{2aq} (ε_β) (Deines et al., 1974; Mook et al., 1974). Then, making the (1) explicit with respect to $\delta^{13}C_{CO2}$, the carbon isotopic composition of the CO_2 gas phase in equilibrium with the collected waters can be written as:

$$\delta^{13}C_{CO2} = \delta^{13}C_{TDIC} - [\varepsilon_\alpha * \chi HCO_3 + \varepsilon_\beta \chi CO_2] \qquad (2)$$

The results listed in Table 5 show a narrow range of isotopic ratios (-13.5±2.4‰) for the pristine CO_2 gas dissolved in most of the samples including both thermal and cold waters, with some exceptions made by lower values both for some cold waters (ranging from -19 to -21‰) and a

thermal water (-23‰ for Repole spring), or higher values (-7‰) of one thermal and one cold sample (18 and 36, respectively). Considering that $\delta^{13}C$ values of sedimentary C vary significantly and could originate from two major sources of marine limestone, including slab carbonate ($\delta^{13}C$ = 0‰; Hoefs, 1980) and organic C from sedimentary rocks ($\delta^{13}C$ normally lower than - 20‰; Hoefs, 1980) we argue that the calculated isotopic values denote a provenance of pristine CO_2 from the sedimentary rocks. In any case, the results exclude a massive contribution to the deep-gas phase of organic and mantle-derived CO_2, the former typically marked by $\delta^{13}C$ from-70‰ to-25‰, the latter by $\delta^{13}C_{MORB}$ = - 6.5‰ (Faure, 1986; Javoy et al., 1986; Sano and Marty, 1995).

4.6 Helium isotopes

The origin of the CO_2-dominated gases dissolved in the sampled waters can be traced using the isotopic composition of the dissolved helium. In fact, helium comes from three different and well distinguishable sources (mantle, crust and air), each marked by different isotopic ratios (e.g. Ozima and Podosek, 2002) and thus useful for evaluating different geological environments (Mamyrin and Tolstkhin, 1984; Ozima and Podosek, 2002). He-isotope ratios have been used in several tectonically active sections of the Apennine chain to identify deep gas sources in the North-Central Apennines (Minissale et al., 1997; Minissale et al., 2004), mantle-derived products intruded at shallow levels in the crust in Southern Apennines (Italiano et al. 2000) or, contrastingly, to exclude the contribution of mantle-derived products in CO_2-rich fluids of Central Apennines (Italiano et al., 2008). It was considered that the genesis of the fluids circulating over the tectonically active area of the Southern Apennine is closely related to the role of the faults as a preferential escape route for the very mobile helium and also possible ways to allow mantle fluids to intrude and raise towards shallower crustal levels. $^3He/^4He$ values have been measured in almost all the dissolved gases; the recorded Ra values (Ra = atmospheric helium isotope ratio = $1.39x10^{-6}$) range from 0.12 to 0.88 Ra for the cold waters and from 0.05 to 0.33 Ra for the thermal waters. The logarithmic graph of Figure 8 shows the distribution of the helium isotopic ratios (normalized to the atmosphere) versus

the $^{4}He/^{20}Ne$ ratio. The mixing lines on the graph refer to binary mixings among the possible helium sources ($^{3}He/^{4}He$ end members: air = 1 Ra; radiogenic helium= 0.01 Ra; mantle-derived helium= 6.5 Ra, i.e. the average value for the European Subcontinental Mantle; Dunai and Baur, 1995). The considered He/Ne end-members are: air = 0.318; ASW = 0.285; Crust = Mantle > 1000). The helium isotope data of the cold waters fall close to the atmosphere-crust mixing line and have broadly higher ^{3}He contents than the thermal waters. The Figure 8 plot suggests a mixing of crustal-originated and atmospheric-derived helium for the dissolved gas phase over the whole study area.

The CO_2-^{3}He-^{4}He ternary plot (Figure 9) show all the samples with the advantage that binary mixing relationships can be easily recognized by straight trajectories. Most of the gases extracted from the cold waters fall on a linear trajectory joining the CO_2 apex to the pure ^{4}He axis, while most of those coming from the thermal waters fall on the ^{4}He axis. The two lines on the graph underline the influence of CO_2 loss and air contamination on the pristine gas phase interacting with the groundwaters and well agree with the considerations already made for the chemistry of the dissolved gases. Moreover, it provides the basic information that the helium dissolved in the thermal waters is mainly made by the heavier isotope (^{4}He) of typical crustal origin.

The relative contribution of the three helium components estimated for all the samples are listed on Table 6 (a, b). Although we do not rule out possible, minor, contribution of ^{3}He of mantle origin, the results display a radiogenic signature for the helium dissolved in the thermal waters (sometimes above 90%), while the cold waters are characterized by a significant contribution from the atmosphere in agreement with the results shown in Figure 8

Bearing in mind that the whole study area is characterized by low heat flow values (Cataldi et al., 1995) and is crossed by several tectonic lines, we argue that, besides helium released by the normal Earth's degassing (O'Nions and Oxburg, 1983), a large amount of radiogenic-type helium feeds the circulating waters. In fact, contamination by atmospheric-type helium comes from the infiltrating waters (normally equilibrated with the atmosphere). However, the evidence that the thermal waters have no significant amounts of atmospheric-type helium implies significant contributions of helium

with a radiogenic signature, probably released as a consequence of the stress application on the host rocks by long-lasting deformative effects.

5 – Discussion and Conclusions

The first data-set containing chemical and isotopic fluid data (waters and gases) taken from 44 different sites over one of the most hazardous seismic areas of the Apennine chain is reported here together with inferences on the origins and interactions of the circulating fluids.

The chemical compositions of the waters reflects different types and degrees of water-rock interactions. Due to the geological complexity of the Calabria Region, and taking into account the different hydro-geological paths recognised in the area, numerous geochemical families have been found: Ca-HCO_3, Na-HCO_3, Ca-SO_4, Na-SO_4 and Na (Ca)-Cl (SO_4). Apart from the chemistry, both thermal and cold waters display a large variability in the physical-chemical parameters, probably driven by different geochemical processes (i.e. water-rock interaction, mixing between aquifers, dissolution of gases of different origins, repeated gas-water interactions, etc.) that affect the water's final features.

All the collected samples are made up of both cold and thermal waters from which the dissolved gases were extracted. The dissolved gas phase is always the result of gas-water interactions that occur when a deep-originated CO_2-dominated gas interacts with the groundwaters; large extents of CO_2 dissolution are a consequence of prolonged gas-water interactions, mainly occurring for the thermal waters, characterized by an N_2-dominated dissolved gas phase. The high concentrations of low soluble helium rule out the possibility that degassing processes affected the gas composition.

The low heat flow of the study area, excluding widespread contributions from magmas intruded in shallow crustal levels, also provides useful indications on constraining the origin of the dissolved gases. In agreement with the heat flow data, the isotopic signature of the dissolved helium denotes a major contribution of radiogenic-type helium to the thermal waters. The gas phase exhibits a typical crustal origin with a large contribution of radiogenic products. Contrastingly, contamination by

atmospheric-derived helium are found, as expected, in the dissolved gases of the cold waters. Starting from a common atmospheric helium content for all the infiltrating waters, the different $^{3}He/^{4}He$ ranges of thermal and cold waters are explained as a consequence of significant admixture of radiogenic helium due to the long residence time of the thermal waters. Radiogenic helium (Ra = 0,02) is produced by the radioactive decay of radionuclides enriched in granites and metamorphic rocks that represent a very common lithology throughout the study area. We propose that a long-lasting rock deformation activity provides the necessary stress to the rocks to release the trapped helium. Information from geodetic surveys reveals that deformation of the Calabrian arc occurs at a rate in the order of 3.0 ± 0.6 mm yr−1, 2.0 mm yr−1 of which are accommodated on land (Serpelloni et al., 2007).

The low heat flow (Cataldi et al., 1995) of the whole Calabria Region that rules out the uprising of magma bodies or the presence of magma intrusions at shallow depth in the crust, implies that the thermal character of the investigated waters is a consequence of the deepening of the hydrological circuit in fractured areas marked by a normal geothermal gradient (~30°C/km) allowing the existence of low to medium-enthalpy aquifers at a depth of about 4-6 km. For some of the thermal waters the temperatures calculated by different geothermometers show a limited cooling as a result of a fast uprise through highly permeable discontinuities, namely the local faults. For this area the tectonic setting-thermal waters relationship looks much tighter to the respect of other seismic areas of Southern Apennines, normally characterized by an anomalous thermal flux related to diffuse volcanism.

Intense fault-fluid relationships can be found in some of the investigated sites: the chemical and isotopic composition of both thermal and cold waters related to the Strongoli-Cerenzia line (Fig. 1) shows how the cold waters of Casabona, Strongoli and Verzino (samples 32, 44, 45-46, respectively) follow the broad E-W fault trend in contrast to the thermal waters (Cerenzia, Cotronei and Repole spring; samples 8, 9-14, 23-24, respectively) that are aligned along a broad N-S trend

crossing the area hit by the destructive earthquake occurred on May 8th, 1638. The crossing area is located between the Vette and the Strongoli-Cerenzia lines (Fig. 1).

A further example is given by the waters sampled at the Gioa Tauro Plain that seem to be driven by the Nicotera-Gioiosa Jonica Line. That fault borders the northern area of the plain and clearly separates the two groups of waters: the thermal waters are mostly discharged close to the fault trend (thermal wells of Nicotera, S. Calogero, Laureana di Borrello and Rosarno), while cold waters, spread over the whole area, are mostly aligned on a subparallel trend (see the box in Figure 1). The evidence that the uprising and the circulation of the fluids is fault-dependent, coupled with the presence of several seismogenic regional faults (Basili et al, 2008) responsible for the destructive shocks in 1783 and 1905 (Figure 1) highlights the role of the faults in driving the circulating fluids and the catastrophic seismic events. As Northern and Southern Calabria have no longer been affected by major earthquakes for 130 and 90 years, respectively, and probably more than in other seismic areas around the world, the seismicity exhibits strong irregularities in its time patterns, any probabilistic model for possible forecasting of impending earthquakes results quite unreliable. Indeed, the development of any tool aimed at the reduction of the seismic risk for the area would be useful, and a geochemical monitoring of the fluids seems to be a promising tool to be developed. Our data show that the chemical composition of some repeatedly collected samples did not change very much over a time span of more than ten years. Although the collected data are insufficient to discriminate seasonal variations and/or the occurrence of modifications induced by other reasons (i.e. anthropogenic), the proposed results may represent a starting point for developing the required long-term monitoring of the circulating fluids.

Acknowledgments.

The research work was supported by the INGV-DPC grants, S2-project, UR2.9-Italiano and V5-project, UR9-Italiano. The authors are indebted to Luana Gallo, Andrea De Filippis and Carmine Caratozzolo from the Department of Ecology of Università della Calabria for their crucial help in

the sample collection and field measurements. The manuscript greatly benefited from critical reviews and suggestions of Karen Brauer and an anonymous reviewer.

References

Ambrosetti, P., Bosi, C., Carraio, F., Ciaranfi, N., Panizza, M., Papani, G., Mezzani, L., Zanferrari, A., 1987. Neotectonic Map of Italy. Quad. Ric. Sci., 114, 4.

Amodio Morelli, L., Bonardi, G., Colonna, V., Dietrich, D., Giunta, G., Ippolito, F., Liguori, V., Lorenzoni, S., Paglionico, A., Perrone, V., Picarretta, G., Russo, M., Scandone, P., Zanettin-Lorenzoni, E., Zappetta, A., 1976. L'arco calabro-peloritano nell'orogene appenninico-magrebide. Mem. Soc. Geol. It., 17, 1-60. (In Italian).

Arnórsson, S., Gunnlaugsson, E., Svavarsson H., 1983. The chemistry of geothermal waters in Iceland. III. Chemical geothermometry in geothermal investigations. Geochimica et Cosmochimica Acta, 47, 567-577. doi:10.1016/0016-7037(83)90278-8

Basili, R., Valensise, G., Cannoli, P., Burrato, P., Fracassi, U., Mariano, S., Tiberti, M., Boschi, E., 2008. The Database of Individual Seismogenic Sources (DISS), version 3: Summarizing 20 years of research on Italy's earthquake geology. Tectonophysics, 453, 20-43. doi:10.1016/j.tecto.2007.04.014

Boschi, E., Guidoboni, E., Ferrari, G., Mariotti, D., Valensise G., Gasperini P. (Eds). 2000. Catalogue of Strong Italian Earthquakes. Ann. Geofis., 43, 268 pp.

Bosi, C., Carobene, L., Sposato, A., 1996. Il ruolo dell'eustatismo nella evoluzione geologica nell'area mediterranea. Memorie Società Geologica Italiana 51, 363-382.

Capasso, G., Inguaggiato, S., 1998. A simple method for the determination of dissolved gases in natural waters. An application to thermal waters from Vulcano island. Appl. Geoch., 13, 631-642 doi:10.1016/S0883-2927(97)00109-1.

Caracausi, A., Italiano, F., Martinelli, G., Paonita, A., Rizzo A., 2002. Long-term geochemical monitoring in seismically active areas of Italy: implications for seismic hazard reduction.

XXVIII General Assembly of the European Seismological Commission, Genova (Italy), 1-6 September 2002

Caracausi, A., Italiano, F., Martinelli, G., Paonita, A., Rizzo A., 2005. Long-term geochemical monitoring and extensive/compressive phenomena: case study of the Umbria region (Central Apennines, Italy). Annals of Geophysics, 48, 43-53.

Castello B, Selvaggi G., Chiarabba C, Amato A. (2006) CSI, Catalogo della sismicità italiana 1981-2002, versione 1.1, INGV-CNT Roma. http://www.ingv.it/CSI/

Catalano S., De Guidi G., Monaco C., Tortorici G., Tortorici L., 2008. Active faulting and seismicity along the Siculo-Calabrian Rift Zone (Southern Italy). Tectonophysics, 453, 177-192. doi :10.1016/J.TECTO.2007.05.008

Cataldi, R., Mongelli, F., Squarci, P., Taffi, L., Zito, G., Calore C., 1995. Geothermal ranking of Italian territory - Geothermics, 24, 115-129. doi:10.1016/0375-6505(94)00026-9

Deines, P., Langmuir, D., Harmon, R.S. 1974. Stable carbon isotope ratios and the existence of a gas phase in the evolution of carbonate groundwaters. Geochim. Cosmochim. Acta, 38, 1147-1164, doi:10.1016/0016-7037(74)90010-6.

Dumas, B., Gueremy, P., Raffy, J. 2005. Evidence for sea-level oscillations by the 'characteristic thickness' of marine deposits from raised terraces of Southern Calabria (Italy). Quaternary Science Reviews, 24, 2120-2136, doi: 10.1016/j.quascirev.2004.12.011.

Dunai, T.J., Baur, H., 1995. Helium, neon and argon systematics of the European subcontinental mantle: implications for its geochemical evolution. Geochim. Cosmochim. Acta 59, 2767-2783 doi:10.1016/0016-7037(95)00172-V

Epstein, S., Mayeda, T. 1953. Variation of O content of water from natural sources, Geochim. Cosmochim. Acta 4, 213–224. doi:10.1016/0016-7037(53)90051-9

Fouillac, C., Michard, G., 1981. Sodium/lithium ratio in water applied to geothermometry of geothermal reservoir, Geothermics 10, 55-70

Faure G., 1986. Principles of isotope geology. Wiley New York, 2nd Edition, 589 pp.

Fournier, R.O., 1977. A review of chemical and isotopic geothermometers for geothermal systems. In: Proceedings of the Symp. on Geotherm. Energy. Cento Scientific Programme, Ankara, pp. 133-143.

Fournier, R.O., Truesdell, A.H., 1973. An empirical Na-K-Ca geothermometers for natural waters. Geochim. Cosmochim. Acta 37, 1255–1279. doi:10.1016/0016-7037(73)90060-4

Fournier, R.O., Potter, R.W., 1979. Magnesium correction to the Na-K-Ca chemical geothermometer. Geochim. Cosmochim. Acta 43, 1543-1550. doi:10.1016/0016-7037(79)90147-9

Gat, J.R., Carmi, I., 1970. Evolution in the isotopic composition of atmospheric waters in the Mediterranean Sea area. J. Geophys. Res. 75, 3039-3048.

Ghisetti, F., Vezzani, L., 1982. Different styles of deformation in the Calabrian Arc (southern Italy): implications for a seismotectonic zoning. Tectonophysics, 84, 149-165. doi:10.1016/0040-1951(82)90101-9

Giggenbach, W.F., 1988. Geothermal gas equilibria. Derivation of Na-K-Mg-Ca geoindicators. Geochim. Cosmochim. Acta 52, 2749-2765. doi:10.1016/0016-7037(80)90200-8

Giggenbach, W.F., Corrales, R.S., 1992. The isotopic and chemical compsition of waters and steam discharges from volcanic-magmatic-hydrothermal systems of the Guanacoste Geothermal Province, Costa Rica. Applied Geochemistry, 7, 309-322 doi:10.1016/0883-2927(92)90022-U

Gruppo di lavoro CPTI, 2004. Catalogo parametrico dei terremoti italiani, versione 2004 (CPTI04), INGV, Bologna. http//emidius.mi.ingv.it/CPTI04

Hartmann, J., Levy J.K., 2005. Hydrogeological and Gasgeochemical Earthquake Precursors. A Review for Application. Natural Hazards, 34, 279-304. DOI: 10.1007/s11069-004-2072-2

Hilton, D.R., 1996. The helium and carbon isotope systematics of a continental geothermal system: results from monitoring studies at Long Valley caldera (California, U.S.A.). Chemical Geology, 127, 4, 269-295. DOI: 10.1016/0009-2541(95)00134-4

Hoefs, J., 1980. Stable Isotope Geochemistry. Springer. Berlin, 208 pp.

Italiano, F., Martelli, M., Martinelli, G., Nuccio, P.M., 2000. Geochemical evidence of melt intrusions along lithospheric faults of the Southern Apennines, Italy: Geodynamic and seismogenic implications. Jour. Geoph. Res., 105, B6, 13569-13578

Italiano, F., Martinelli, G., Nuccio, P. M., 2001. Anomalies of mantle-derived helium during the 1997-1998 seismic swarm of Umbria-Marche, Italy, Geophys. Res. Lett. Vol. 28 , No. 5 , p. 839-842.

Italiano, F., Martinelli, G., Rizzo, A., 2004. Geochemical evidence of seismogenic-induced anomalies in the dissolved gases of thermal waters: a case study of Umbria (Central Apennines, Italy) both during and after the 1997-1998 seismic swarm. G-Cubed, vol. 5, 11, doi:10.1029/2004GC000720.

Italiano, F., Martinelli, G., Pizzullo, S., Plescia, P., 2007. Greenhouse gases released from the Apennine Chain, Italy: mechanochemical production besides mantle-derived contribution. Invited talk at ICGG9 Taiwan, 1-8 October 2007, Progr. Proceedings, 84

Italiano, F., Martinelli, G., Plescia, P., 2008. CO_2 degassing over seismic areas: the role of mechanochemical production at the study case of Central Apennines. Pageoph, Vol. 165, 1, 75 – 94, DOI: 10.1007/S00024-007-0291-7

Italiano, F., Bonfanti, P., Ditta M., Petrini R., Slejko F., 2008. Helium and carbon isotopes in the dissolved gases of Friuli region (NE Italy): geochemical evidence of CO_2 production and degassing over a seismically active area. Chem Geology, submitted.

Javoy, M., Pineau, F., Delorme, H., 1986. Carbon and nitrogen isotopes in the mantle. Chem. Geol. 57 (1-2), 41-62. doi:10.1016/0009-2541(86)90093-8

Jenny, S., Goes, S., Giardini, D., Kahle, H.G., 2006. Seismic potential of southern Italy. Tectonophysics 415, 81-101. doi:10.1016/j.tecto.2005.12.003

Kharaka, Y.K., Specht, D.J., Carothers, W.W., 1985. Low to intermediate subsurface temperatures calculated by chemical geothermometers. Bulletin of the American Association Of Petroleum Geologists, 69 (2), 273.

Kharaka, Y.K., Mariner, R.H., 1989. Chemical geothermometers and their application to formation waters from sedimentary basins, *in* Thermal History of Sedimentary Basins, Methods and Case Histories, Naeser, N.D., and McCulloh, T.H., eds.: Springer-Verlag, New York, NY, p. 99-117.

Kendall, C., Coplen ,T.B., 1985. Multisample conversion of water to hydrogen by zinc for stable isotope determination. Anal. Chem., 57, 1437-1440. DOI: 10.1021/ac00284a058

King, C.Y., 1986. Gas geochemistry application to earthquake prediction: an overview, J. Geophys. Res., 91, 12,269–12,289.

Longinelli, A., Selmo, E., 2003. Isotopic composition of precipitation in Italy: a first overall map. Journal of Hydrology 270, 75-88, doi:10.1016/S0022-1694(02)00281-0

Mamyrin, B. A., Tolstikhin, I. N., 1984. Helium Isotope in Nature. Elsevier, Amsterdam, 273 pp.

Martinelli, G., 1997. Non seismometrical precursors observations in Europe:steps of earthquake prediction research, in Proceedings of the Workshop"Historical Seismic Instruments and Documents: a Heritage of Great Scientific and Cultural Value" Conseil de l'Europe, Cahiers du Centre Européenne de Geodinamique et de Séismologie, Vol 13,195-216. Walferdange, Luxembourg

Mattei, M., Cifelli, F., D'Agostino, N., 2007. The evolution of the Calabrian Arc: Evidence from paleomagnetic and GPS observations. Earth and Planetary Science Letters 263, 259-274. DOI: 10.1016/j.epsl.2007.08.034.

Minissale, A., 2004. Origin, transport and discharge of CO_2 in central Italy. Earth Science Reviews, 66, 89-141. DOI: 10.1016/j.earscirev.2003.09.001

Minissale, A., Evans, W., Magro, G., Vaselli, O., 1997. Multiple source components in gas manifestations from northcentral Italy. Chem. Geol. 142, 175–192. doi:10.1016/S0009-2541(97) 00081-8

Mook, W.G., Bommerson, J.C., Staverman, W.H., 1974. Carbon isotope fractionation between bicarbonate and gaseous carbon dioxide, Earth Plan. Sci. Lett. 22, 169–176. doi:10.1016/0012-821X(74) 90078-8

Moretti, A., Guerra, I., 1997. Tettonica dal Messiniano ad oggi in Calabria: implicazioni sulla geodinamica del sistema Tirreno Arco-Calabro. Boll.Soc.Geol.It, 116, 125-142. (In Italian).

Ogniben, L., 1969. Schema introduttivo alla geologia del confine Calabro-lucano. Mem.Soc.Geol.It., 8, 453-763. (In Italian).

O'Nions, R.K.. Oxburgh, E.R., 1983. Heat and helium in the Earth. Nature 306, 429-431. DOI: 10.1038/306429a0.

Ozima, M., Podosek., F.A., (2002). Noble Gas Geochemistry: Cambridge University Press. Cambridge, UK, 286 pp.

Parkhurst, D.L., Appelo, C.A.J., 1999. User's guide to PHREEQC (version 2) - a computer program for speciation, reaction-path, 1D-transport, and inverse geochemical calculations. US Geol. Surv. Water Resour. Inv. Rep. 99 - 4259, 312 pp.

Pizzino, L., Burrato, P., Quattrocchi, F., Valensise, G., 2004. Geochemical signatures of large active faults: the example of the 5 February 1783, Calabrian Earthquake. J. of Seismology 8, 3, 363-380. DOI:10.1023/B:JOSE.0000038455.56343.e7

Sano, Y., Wakita, H., 1988. Precise measurement of helium isotopes in terrestrial gases. Bull. Chem. Soc. Jpn. 61, pp. 1153–1157 doi:10.1246/bcsj.61.1153

Sano, Y., Marty, B. 1995. Origin of carbon in fumarolic gas from island arc, Chem. Geol., 119, 265–74. doi:10.1016/0009-2541(94)00097-R

Serpelloni, E., Vannucci, G., Pondrelli, S., Argnani, A., Casula, G., Anzidei, M., Baldi, P., Gasperini, P., 2007. Kinematics of the Western Africa-Eurasia plate boundary from focal mechanisms and GPS data. Geophys. J. Int., 169, 3, 1180-1200 DOI: 10.1111/j.1365-246X.2007.03367.x

Sugisaki, R., Taki, K., 1987. Simplified analyses of He, Ne, and Ar dissolved in natural waters, Geochem. J. 21, pp. 23–27.

Tansi, C., Tallarico, A., Iovine, G., Gallo, M.F., Falcone, G., 2005. Interpretation of radon anomalies in seismotectonic and tectonic-gravitational settings: the south-eastern Crati graben (Northern Calabria, Italy). Tectonophysics 396, 181-193. DOI: 10.1016/j.tecto.2004.11.008

Tansi, C., Muto, F., Critelli, S., Iovine, G., 2007. Neogene-Quaternary strike-slip tectonics in the central Calabrian Arc (southern Italy). Journal of Geodynamics 43, 393-414. DOI: 10.1016/j.jog.2006.10.006

Thomas, D., 1988. Geochemical precursors to seismic activity, PAGEOPH., 126, 241–266.

Tortorici, L., 1981. Analisi delle deformazioni fragili postorogene della Calabria settentrionale. Boll. Soc. Geol. It., 100, 291-308. (in Italian).

Tortorici., L., Monaco, C., Tansi, C., Cocina, O., 1995. Recent and active tectonics in the Calabrian Arc (Southern Italy). Tectonophysics, 243, 37-55. doi:10.1016/0040-1951(94)00190-K

Tortorici, G., Bianca, M., De Guidi, G., Monaco, C., Tortorici, L., 2003. Fault activity and marine terracing in the Capo Vaticano area (southern Calabria) during the Middle-Late Quaternary. Quaternary International, 101-102, 269-278. doi:10.1016/S1040-6182(02)00107-6

Toutain, J.P., Baubron, J.C., 1999. Gas geochemistry and seismotectonics: a review, Tectonophysics 304 (1-2),1-27. doi:10.1016/S0040-1951(98)00295-9

Valensise, G., Pantosti, D., 2001. Database of potential sources for Earthquakes larger than M 5.5 in Italy Annali di Geofisica, supplement to vol. 44, 4.

Van Dijk, J.P., Scheepers, P.J.J., 1995. Neotectonic rotations in the Calabrian Arc: implications for a Pliocene-Recent geodynamic scenariofor the Central Mediterranean. Earth-Science Reviews, 39, 207-246. doi:10.1016/0012-8252(95)00009-7

Westaway, R., 1993. Quaternary uplift of Southern Italy. Jour. Geophys. Res., 98 (B12), 21741-21772.

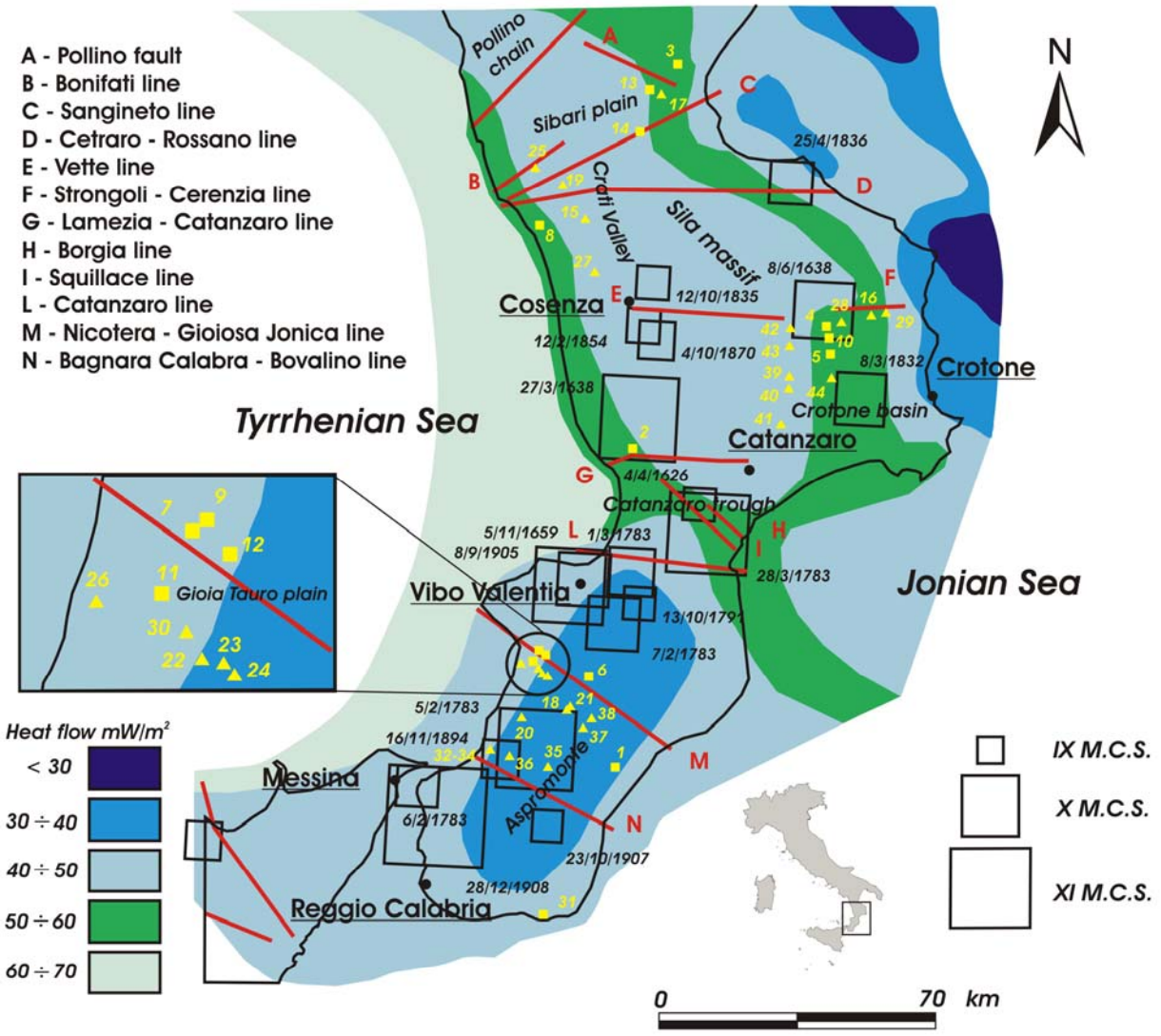

Figure 1 – Location of the sampling sites in the South Apennine seismic-prone area over the heat flow map of the region (after Cataldi et al., 1995). Sample identification numbers refer to Tables 1a and 1b. Squared yellow marks = thermal waters; yellow triangles= cold waters. The main tectonic trends (red lines after Basili et al., 2008) are marked by capital letters and explained on the left-side legend. The intensity of the destructive seismic events of the last centuries (Boschi et al, 2000) is shown by the blank squared marks (width proportional to MCS intensity; see legend on the right-side).

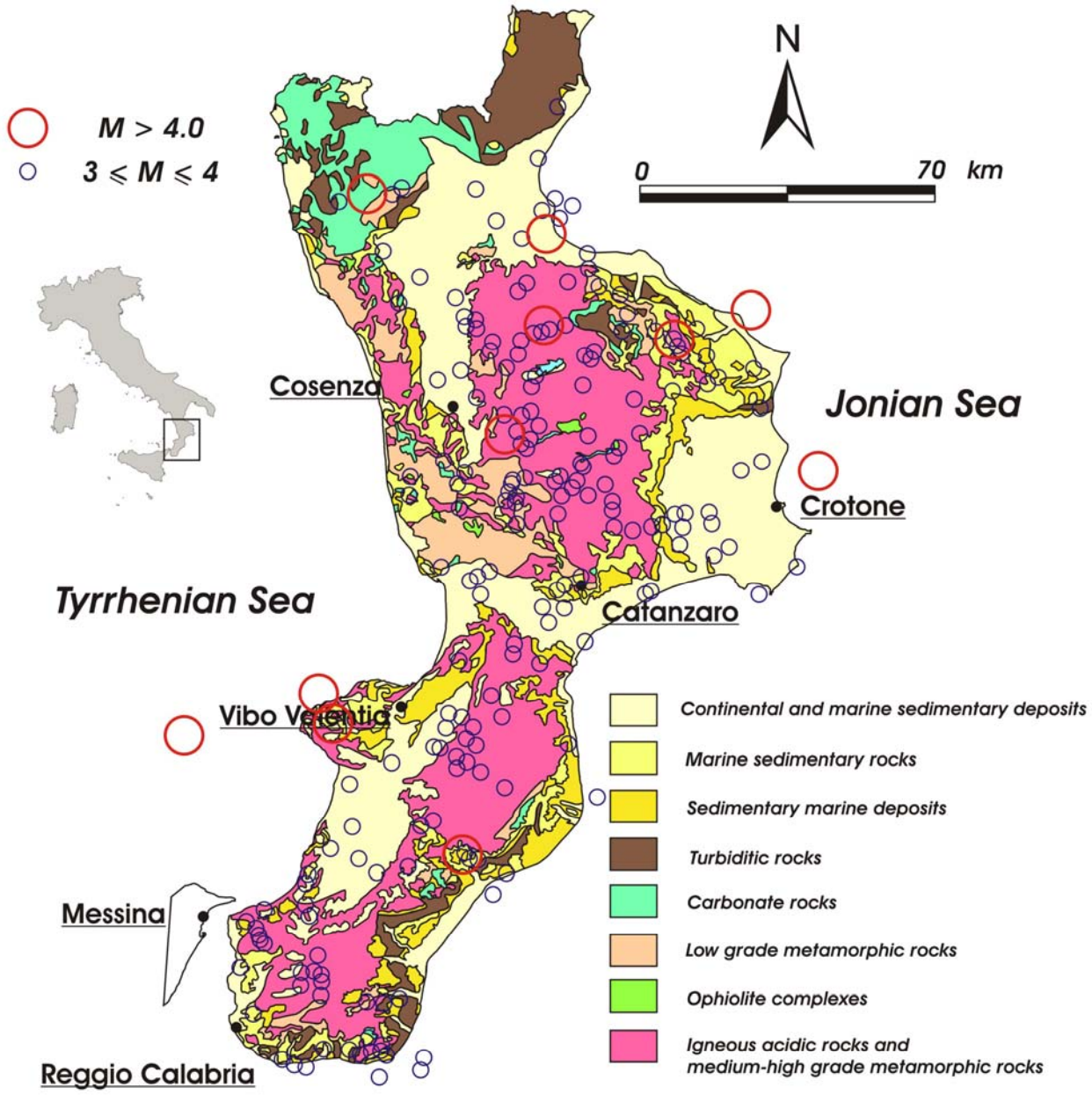

Figure 2 – Sketch map of the geological setting of the study area. The recent seismicity (1980-2005) with M ≥ 3 is also plotted (circles).

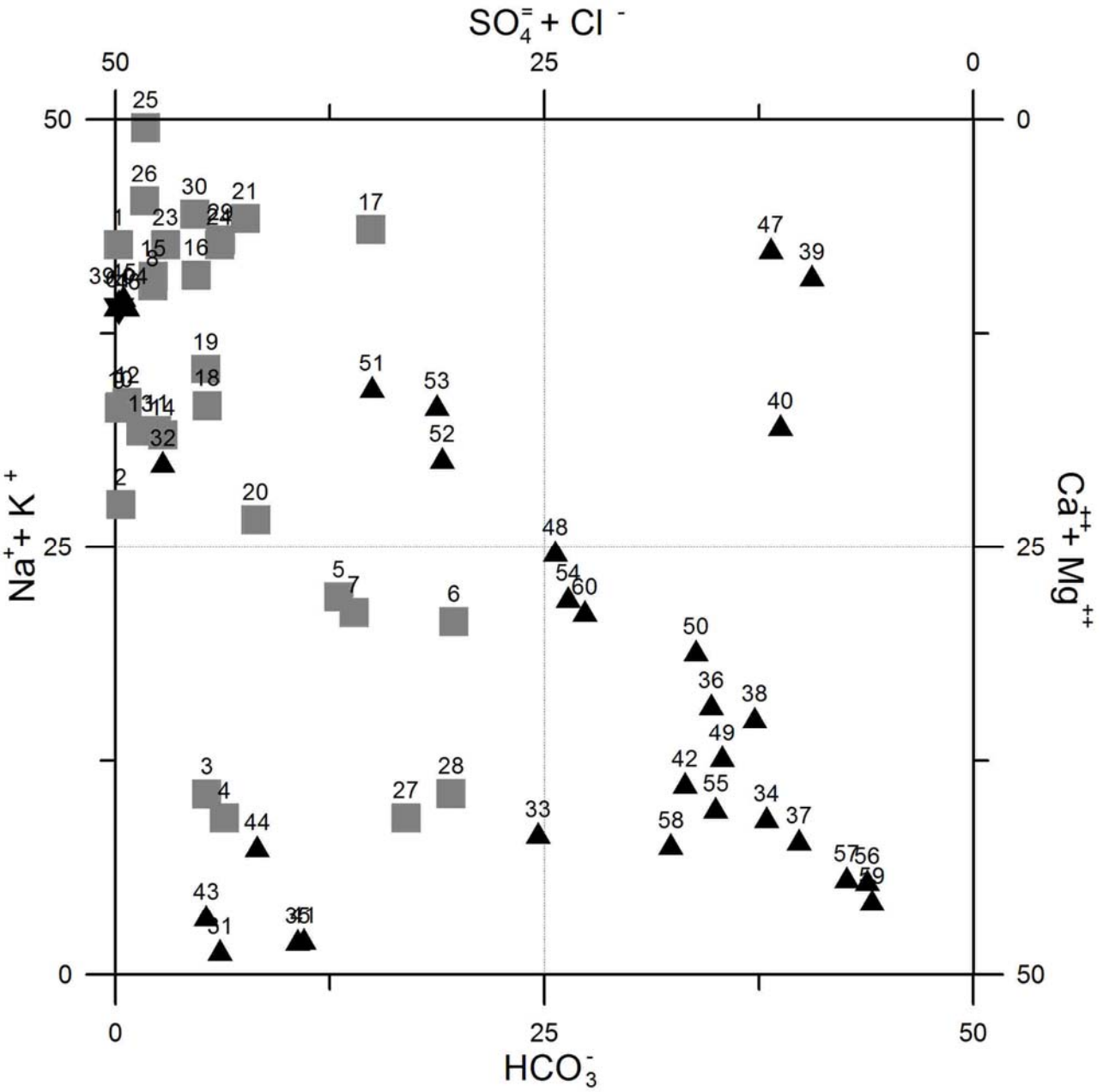

Figure 3 – Langelier-Ludwig diagram of the sampled waters. Black triangles = cold waters; Grey squared marks = thermal waters; black star = seawater.

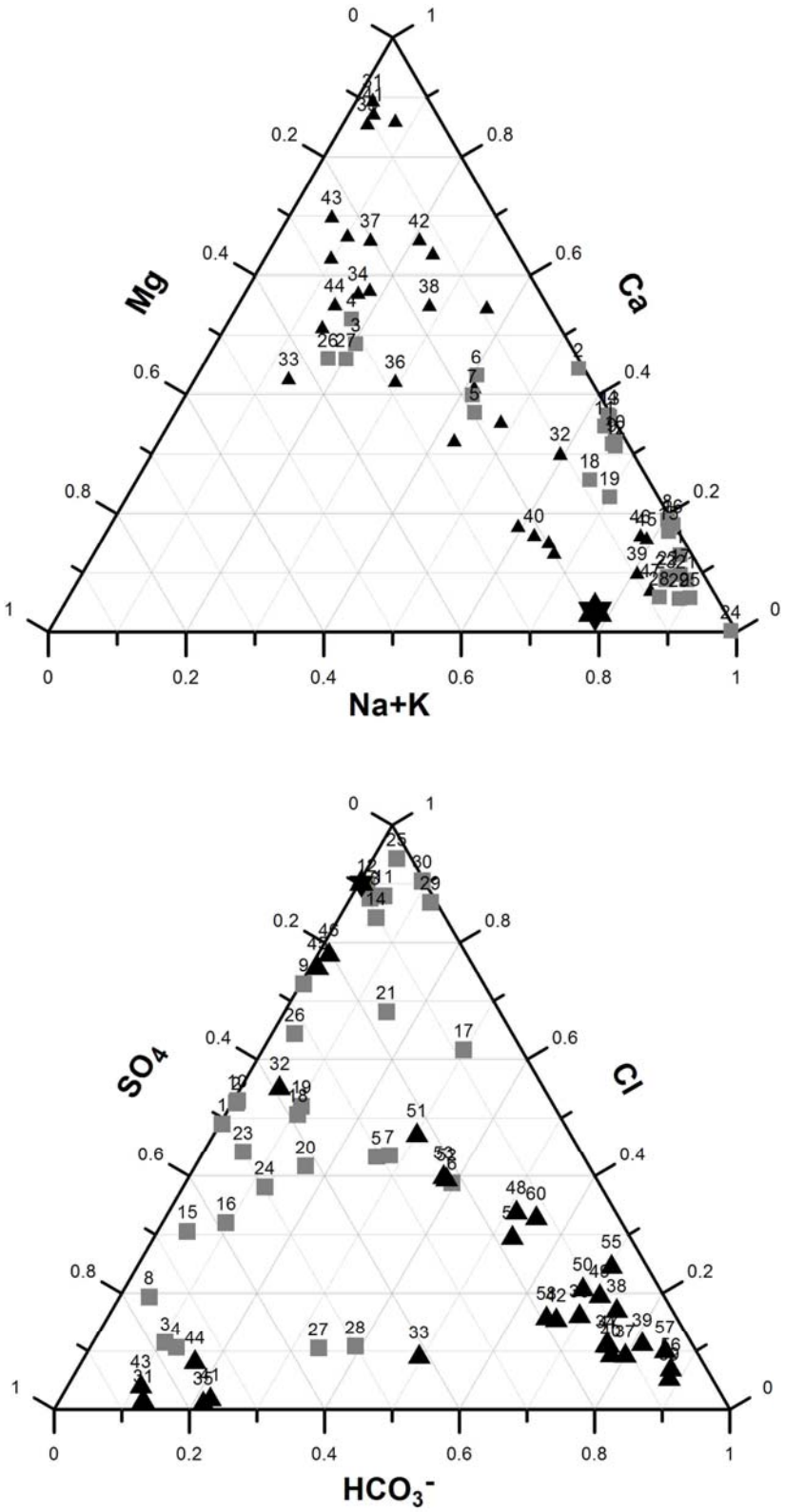

Figure 4 – Ternary diagrams of cations (4a) and anions (4b). Symbols as in Figure 3

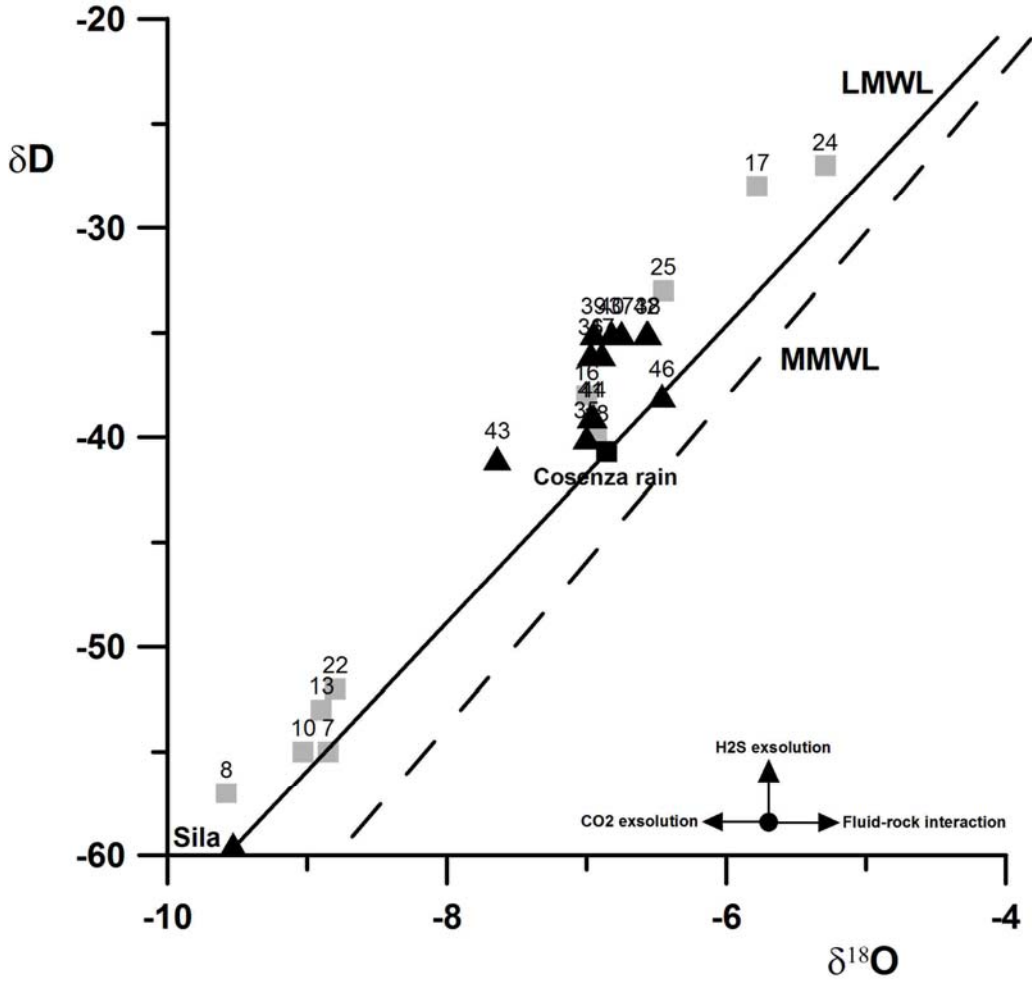

Figure 5 – Oxygen and deuterium isotopes relationship of the water samples**.** In the same Figure the Local Meteoric Water Line (LMWL full line; Longinelli and Selmo, 2003) and the Mean Mediterranean Water Line (MMWL, hatched line; Gat and Carmi, 1970) are reported as an indication for the mean isotopic composition of the infiltrating waters. As reference points, the isotopic composition of a shallow spring discharging in the Sila Massif and the isotopic composition of rain water at Cosenza (central Calabria, Longinelli and Selmo, 2003), are also shown by the black triangle and the squared black marks, respectively. See Figure 3 for symbols explanation; numbers refer to the sample column on Table 2 (a, b).

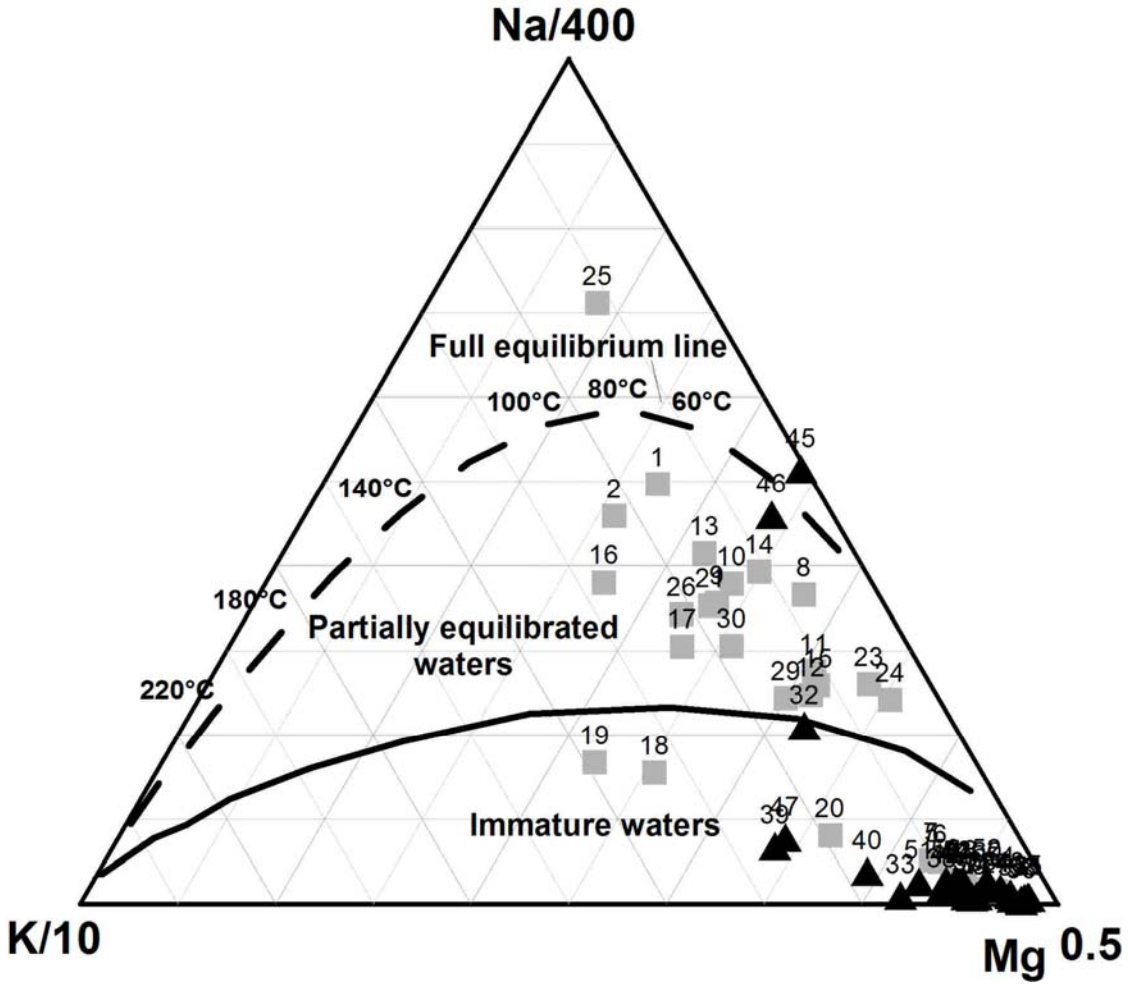

Figure 6 – Na–K–Mg ternary diagram. The diagram provides at-a-glance information on the degree of water–rock equilibrium for low-temperature geothermal systems. (Giggenbach and Corrales, 1992). Although most of the sampled waters fall close to Mg vertex, the plot allows for a clear distinction of the partially equilibrated thermal waters and the immature cold waters into well separated groups. Hatched line indicates the full equilibrium line; the full line indicates the boundary between immature and partially equilibrated waters. Symbols as in Figure 3.

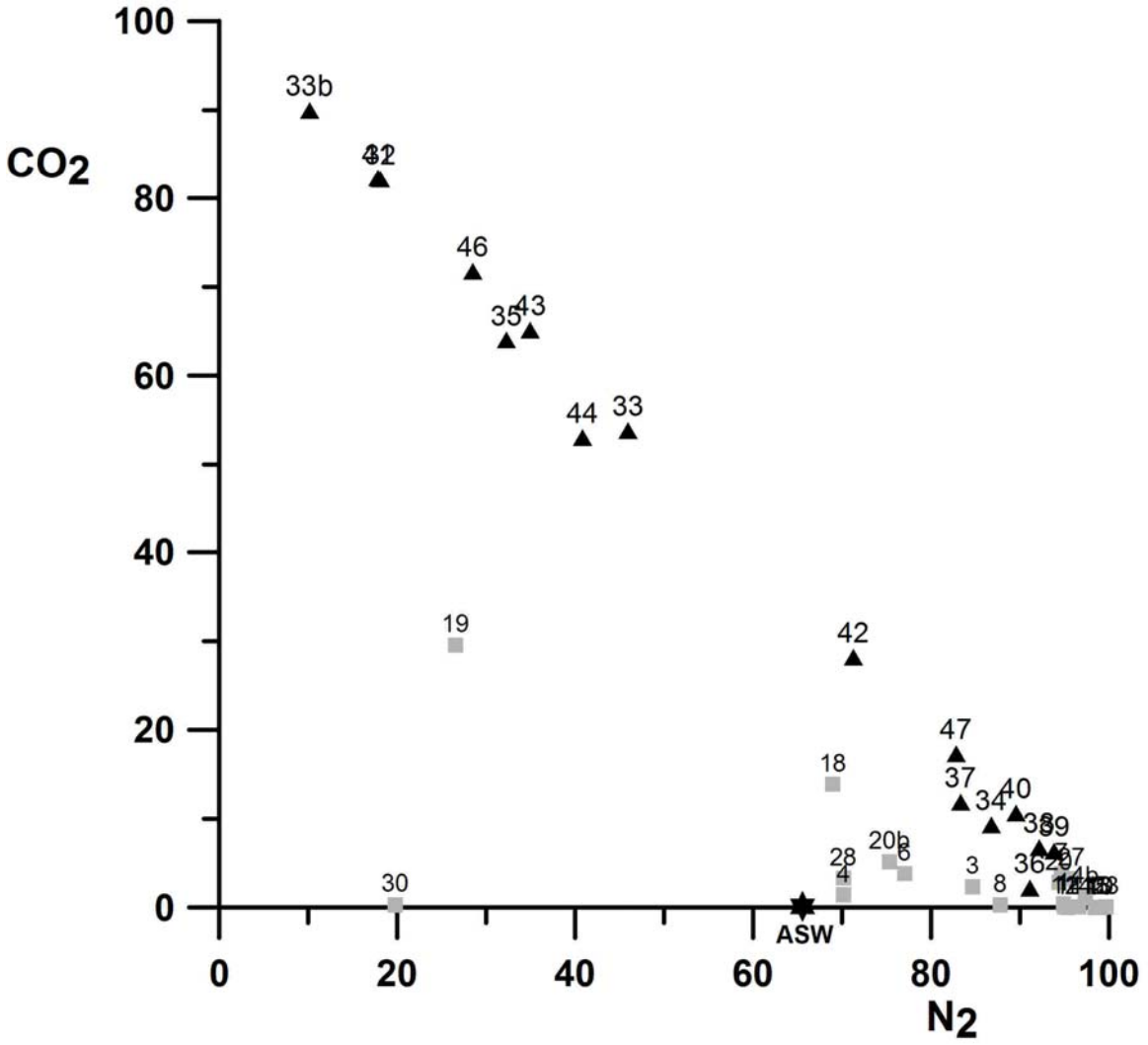

Figure 7 – N_2 versus CO_2 in the dissolved gases. The straight alignment followed by the sample distribution on the graph clearly show how CO_2+N_2 practically represent the total amount of dissolved gases. The Air Saturated Water (ASW) is reported as reference point. See Figure 3 for symbols explanation; numbers refer to sample identification, the first column on Table 4 (a, b)

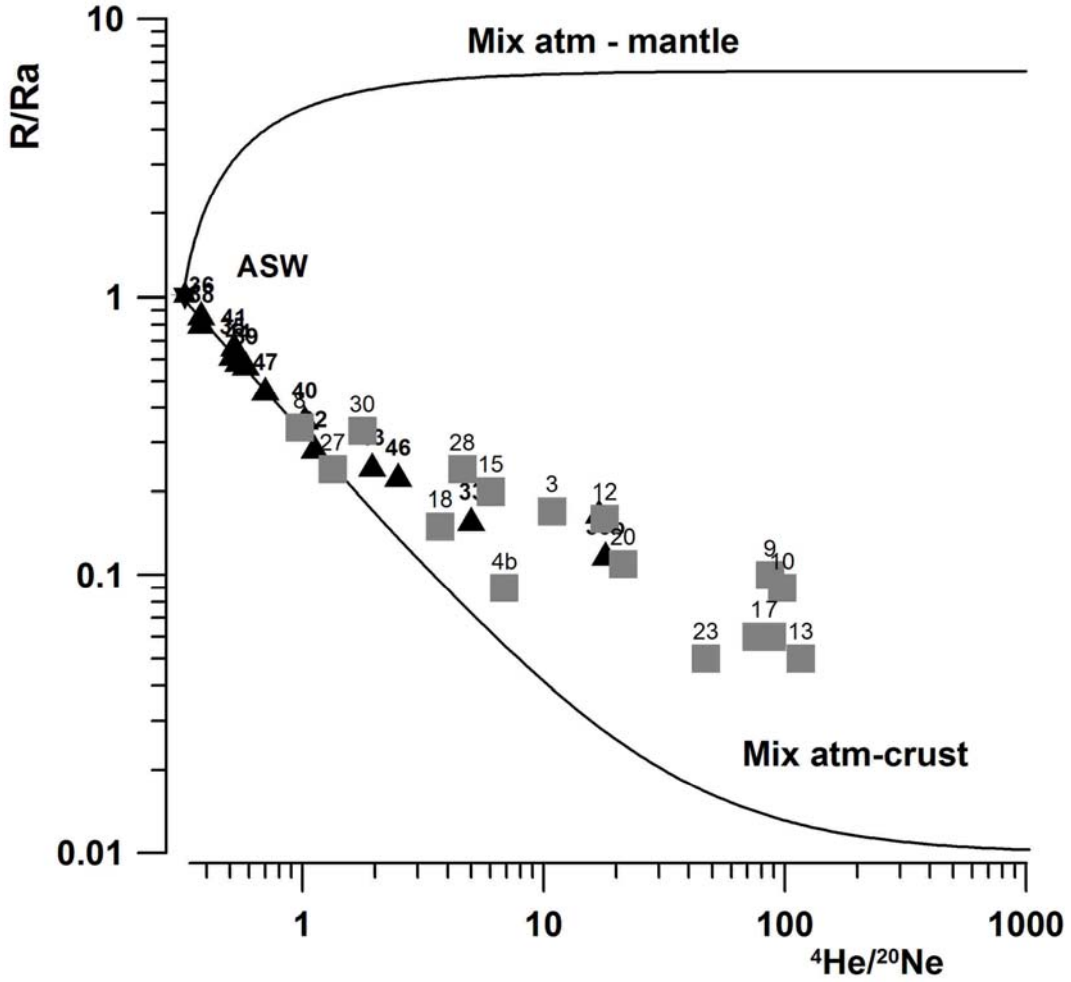

Figure 8 – He/Ne vs. helium isotopic ratios. The dissolved helium is a mixing between the atmosphere and a radiogenic-type end members. The mixing-boundary lines are built with the following end members: atmosphere (as dissolved air) R/Ra =1 and He/Ne = 0.285; Mantle R/Ra = 6.5 and He/Ne = 1000; continental crust R/Ra = 0.01 and He/Ne = 1000. All the $^{3}He/^{4}He$ ratios here expressed as R/R_a; values are corrected for the atmospheric contamination following previously described procedures (e.g. Hilton, 1996). See Figure 3 for symbols explanation; numbers refer to sample identification, the first column in Table 6 (a, b).

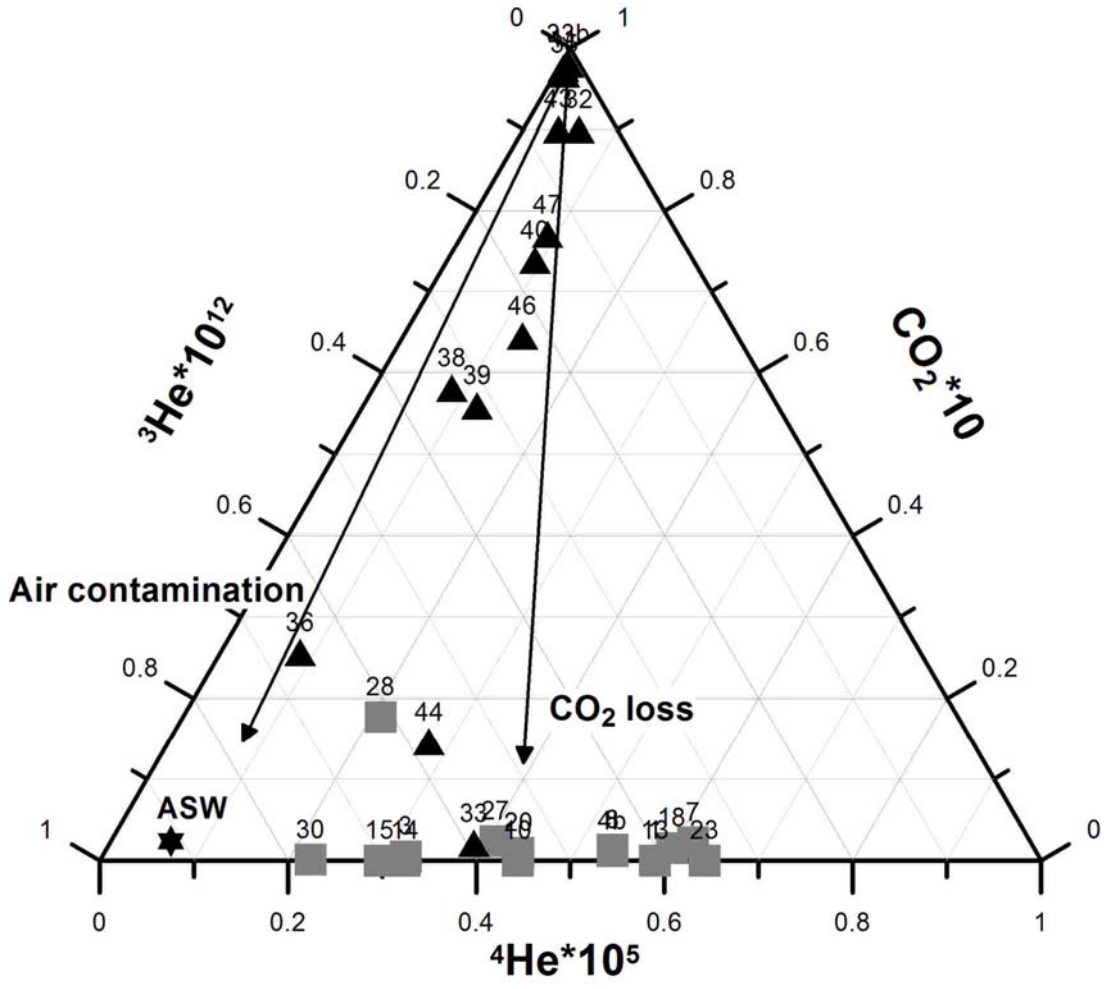

Figure 9 - Ternary plot of CO_2, ^3He, and ^4He of the dissolved gas samples. The vertical line shows the effects of CO_2 loss. The effect of air contamination on dissolved gases is also shown by the line joining the CO_2 apex and the ASW point. Most of the samples denotes that both the processes of CO_2 loss and air contamination modify the pristine gas composition. Almost all the thermal waters fall on the ^3He - ^4He axis showing that CO_2 in the extracted gas phase, is totally lost. See figure 3 for symbols explanation; numbers refer to sample identification, the first column on table 6 (a, b).

Table 1 – Location of the sampling sites and sampling dates. Coordinates in UTM WGS84 units. Table 1a and 1b refer to thermal and cold samples, respectively, listed in alphabetical order. The reported sample numbers (1st column) identify the collected samples on the graphs; the map ID (last column) identifies the site location on the map of Figure 1

Table 1a – Thermal waters

Sample #	Site	Date	Latitude	Longitude	Map ID
1	Antonimine spa	31/10/2001	4235085	604505	1
2	Antonimine spa	29/06/2000	4235085	604505	
3	Caronte spa1	29/10/2001	4314647	608790	2
4	Caronte spa1	27/06/1994	4314647	608790	
5	Cerchiara spa	28/10/2001	4411031	619994	3
6	Cerchiara spa	07/05/1993	4411031	619994	
7	Cerchiara spa	23/01/2007	4411031	619994	
8	Cerenzia spring	14/02/2007	4345256	657573	4
9	Cotronei spring	30/10/2001	4338630	658281	5
10	Cotronei spring	25/01/2007	4338630	658281	
11	Cotronei spring	23/06/1994	4338630	658281	
12	Cotronei well	30/10/2001	4338630	658281	
13	Cotronei well	25/01/2007	4337104	656602	
14	Cotronei well	23/06/1994	4337104	656602	
15	Galatro spa	31/10/2001	4337104	656602	6
16	Galatro spa	08/06/1999	4257840	597920	
17	Laureana di Borrello well	26/06/2000	4264276	585428	7
18	Luigiane spa HT	13/02/2007	4370550	585601	8
19	Luigiane spa HT	29/06/1994	4370550	585601	
20	Luigiane spa LT	13/02/2007	4370550	585601	
21	Nicotera well	26/06/2000	4264494	585668	9
22	Palizzi	6/10/2003	4197675	587607	31
23	Repole spring	20/03/2007	4342602	658006	10
24	Repole spring	10/02/1995	4342602	658006	
25	Rosarno well	03/06/2000	4261486	583956	11
26	S. Calogero well	24/06/2000	4263183	586990	12
27	Sibarite spa	29/10/2001	4404589	613104	13
28	Sibarite spa	07/02/1995	4404589	613104	
29	Spezzano spa	07/02/1995	4393955	610800	14
30	Spezzano spa	29/10/2001	4393955	610800	

Table 1b – Cold waters

Sample #	Site	Date	Latitude	Longitude	Map ID
31	Brugnano sulphur spr	04/05/1993	596903	4372192	15
32	Casabona spring	14/02/2007	668295	4348187	16
33	Cassano spring RS	25/01/2007	613154	4404884	17
34	Cittanova spring	20/03/2007	593072	4250377	18
35	Fagnano spring	13/02/2007	591407	4381257	19
36	Palmi sulphur spr	20/03/2007	580937	4247693	20
37	Polistena spr	20/03/2007	593360	4250429	21
38	Rosarno well 1	20/03/2007	585854	4258823	22
39	Rosarno well 2	20/03/2007	586759	4258691	23
40	Rosarno well 3	20/03/2007	587258	4258414	24
41	S. Agata spring	13/02/2007	584449	4385338	25
42	S. Ferdinando spr	20/03/2007	581074	4261350	26
43	S. Vincenzo spring	23/01/2007	599354	4359056	27
44	Strongoli mine spr	25/01/2007	672150	4348701	28
45	Verzino sulphur spr	08/02/1995	661090	4346357	29
46	Verzino sulphur spr	14/02/2007	661090	4346357	
47	Zippone spring	20/03/2007	585128	4259968	30
48	Aspromonte 1	29/05/2000	573192	4238878	32
49	Aspromonte 2	29/05/2000	574222	4238878	33
50	Aspromonte 3	02/06/2000	576599	4239242	34
51	Aspromonte 4	21/03/2000	588622	4235370	35
52	Aspromonte 5	23/03/2000	579254	4236050	36
53	Aspromonte 6	18/03/2000	594979	4245430	37
54	Aspromonte 7	19/03/2000	596860	4248893	38
55	Sila 1	18/07/1995	653013	4332483	39
56	Sila 2	18/07/1995	653017	4329831	40
57	Sila 3	18/07/1995	651529	4323480	41
58	Sila 4	12/02/1995	652700	4346048	42
59	Sila 5	12/02/1995	652235	4342831	43
60	Sila 6	12/02/1995	658473	4333332	44

Table 2 – Physical-chemical parameters, major and minor elements and isotopic composition of (a) thermal waters (b) cold waters. Electrical conductivity in μS/cm; Eh in mV; ion contents in meq per litre; δD and $\delta^{18}O$ in δ‰ versus the international V-SMOW standard. Sample # as in Table 1. 2a = thermal waters; 2b = cold waters. n.d. = not determined

Table 2a

#	Site	Date	T	pH	Eh	El.Cond.	Ca	Mg	Na	K	HCO_3	Cl	SO_4	NO_3	$\delta^{18}O$	δD
1	Antonimine spa	31/10/2001	34.0	7.70	279	14380	23.47	3.04	153.61	0.73	0.59	85.16	87.91	0.70	n.d.	n.d.
2	Antonimine spa	29/06/2000	35.1	7.73	184	13670	86.87	1.49	107.17	0.77	1.33	113.79	101.00	n.d.	n.d.	n.d.
3	Caronte spa1	29/10/2001	38.6	7.10	-284	2420	14.79	9.44	6.19	0.29	3.20	3.45	23.35	0.07	n.d.	n.d.
4	Caronte spa1	27/06/1994	39.0	6.60	-164	2380	16.75	9.38	5.60	0.25	4.40	3.70	26.50	n.d.	n.d.	n.d.
5	Cerchiara spa	28/10/2001	31.8	7.12	-274	1423	5.23	2.77	6.14	0.18	3.65	6.09	4.29	0.04	n.d.	n.d.
6	Cerchiara spa	07/05/1993	27.5	7.05	-11	1290	5.36	2.00	5.03	0.14	4.55	4.48	2.50	n.d.	n.d.	n.d.
7	Cerchiara spa	23/01/2007	31.3	6.91	-262	2042	5.84	2.70	6.09	0.18	4.00	6.27	4.11	0.01	-8.85	-55
8	Cerenzia spring	14/02/2007	30.7	9.01	-180	1750	2.30	0.06	9.75	0.03	0.50	2.22	8.74	0.01	-9.58	-57
9	Cotronei spring	30/10/2001	29.8	7.97	-300	9080	33.54	2.34	69.89	0.49	0.50	75.40	27.53	0.28	n.d.	n.d.
10	Cotronei spring	25/01/2007	34.1	7.78	-248	10390	25.25	1.16	51.86	0.29	0.45	41.25	36.08	0.01	-9.03	-55
11	Cotronei spring	23/06/1994	31.2	8.51	-217	3560	12.02	0.65	22.02	0.13	1.84	33.77	2.76	n.d.	n.d.	n.d.
12	Cotronei well	30/10/2001	35.2	8.75	n.d.	2780	8.02	0.50	17.07	0.13	0.35	22.93	2.24	0.09	n.d.	n.d.
13	Cotronei well	25/01/2007	35.9	8.59	-287	4230	9.44	0.08	16.50	0.09	0.75	22.33	2.41	0.01	-8.90	-53
14	Cotronei well	23/06/1994	36.1	8.10	-354	2790	10.00	0.13	17.25	0.07	1.65	25.19	3.05	n.d.	n.d.	n.d.
15	Galatro spa	31/10/2001	37.1	8.48	-18	1390	2.22	0.18	10.66	0.07	0.55	3.82	8.12	0.04	n.d.	n.d.
16	Galatro spa	08/06/1999	37.4	8.60	-16	1226	2.10	0.02	9.44	0.10	1.00	3.41	6.23	n.d.	-7.00	-38
17	Laureana di Borrello well	26/06/2000	25.3	8.02	-287	6880	6.72	2.27	60.11	0.67	22.00	45.58	6.31	0.01	-5.78	-28
18	Luigiane spa HT	13/02/2007	40.0	6.42	-366	10990	17.12	5.63	43.83	1.39	7.35	34.79	26.54	0.01	-6.93	-40
19	Luigiane spa HT	04/02/1995	43.6	6.59	-105	7240	17.15	5.26	52.60	1.80	8.60	42.50	30.50	n.d.	n.d.	n.d.
20	Luigiane spa LT	13/02/2007	19.7	6.70	-289	2392	7.44	2.74	11.20	0.39	3.50	8.93	8.98	0.03	-7.16	-45
21	Nicotera well	26/06/2000	28.2	7.95	291	7330	6.81	2.24	68.41	0.51	12.90	58.20	14.25	n.d.	n.d.	n.d.
23	Repole spring	20/03/2007	24.3	7.88	-181	1800	3.75	2.14	34.15	0.12	2.30	17.36	19.59	0.02	-8.80	-52
24	Repole spring	10/02/1995	24.3	8.06	-141	3410	3.05	2.04	29.59	0.09	4.60	14.44	18.86	n.d.	n.d.	n.d.
25	Rosarno well	03/06/2000	26.7	8.22	-64	9740	1.10	3.18	443.13	1.05	16.33	435.06	10.04	n.d.	-5.29	-27
26	S. Calogero well	24/06/2000	29.1	7.84	-153	8970	6.00	4.05	94.23	0.86	3.60	68.12	34.05	n.d.	-6.45	-33
27	Sibarite spa	29/10/2001	25.1	7.40	-188	1114	5.56	4.38	2.12	0.11	4.15	1.29	6.81	0.08	n.d.	n.d.
28	Sibarite spa	07/02/1995	23.4	7.14	35	1208	5.19	3.80	2.28	0.13	4.35	1.21	5.56	n.d.	n.d.	n.d.
29	Spezzano spa	07/02/1995	22.8	7.80	-140	6520	4.04	5.65	58.67	0.55	8.20	58.15	0.55	0.17	n.d.	n.d.
30	Spezzano spa	29/10/2001	21.8	7.57	-5	9580	5.12	4.98	80.50	0.70	7.95	77.70	0.22	n.d.	n.d.	n.d.

Table 2b

#	Site	Date	T	pH	Eh	El.Cond.	Ca	Mg	Na	K	HCO_3	Cl	SO_4	NO_3	$\delta^{18}O$	δD
31	Brugnano sulphur spr	04/05/1993	14.8	6.88	167	2710	33.18	2.99	0.86	0.04	4.45	31.25	0.72	n.d.	n.d.	n.d.
32	Casabona spring	14/02/2007	17.2	6.65	-294	11400	36.65	12.76	71.95	0.77	6.60	66.19	46.17	n.d.	-6.08	-34
33	Cassano spring RS	25/01/2007	18.7	7.10	-210	1237	5.39	5.49	1.70	0.39	6.15	1.19	5.14	0.15	-8.34	-47
34	Cittanova spring	20/03/2007	14.6	7.29	48	189	2.41	1.11	0.69	0.08	3.25	0.49	0.54	n.d.	-6.71	-35
35	Fagnano spring	13/02/2007	14.0	7.02	-10	1818	21.19	2.67	0.86	0.04	5.15	0.38	18.68	n.d.	-7.00	-40
36	Palmi sulphur spr	20/03/2007	16.7	6.59	-115	116	1.03	0.69	0.71	0.07	1.75	0.42	0.35	n.d.	-6.97	-36
37	Polistena spr	20/03/2007	14.6	7.10	84	197	2.79	0.85	0.58	0.08	3.45	0.42	0.46	n.d.	-6.75	-35
38	Rosarno well 1	20/03/2007	17.5	8.20	62	140	1.65	0.51	0.83	0.08	2.25	0.53	0.24	n.d.	-6.56	-35
39	Rosarno well 2	20/03/2007	20.0	8.05	n.d.	276	0.55	0.51	4.38	0.24	4.45	0.64	0.39	n.d.	-6.95	-35
40	Rosarno well 3	20/03/2007	20.6	7.82	73	243	0.79	1.01	2.98	0.20	3.80	0.48	0.62	n.d.	-6.82	-35
41	S. Agata spring	13/02/2007	12.5	6.67	-3	2288	30.27	3.14	1.22	0.07	7.45	0.76	25.68	0.01	-6.97	-39
42	S. Ferdinando spr	20/03/2007	17.3	7.18	-9	300	4.57	0.90	1.44	0.10	4.50	1.08	1.20	0.08	-6.57	-35
43	S. Vincenzo spring	23/01/2007	15.2	6.84	-238	2446	27.06	9.21	2.38	0.12	4.05	1.70	32.43	n.d.	-7.64	-41
44	Strongoli mine spr	25/01/2007	17.0	6.32	-264	3880	27.25	15.12	6.88	0.36	8.20	4.26	37.07	n.d.	-6.95	-39
45	Verzino sulphur spr	08/02/1995	17.7	6.76	-119	28800	54.99	17.50	272.10	0.04	3.69	297.00	89.41	n.d.	n.d.	n.d.
46	Verzino sulphur spr	14/02/2007	17.6	6.72	-322	31100	53.31	18.67	252.54	0.50	4.65	252.95	64.89	0.01	-6.46	-38
47	Zippone spring	20/03/2007	21.4	8.26	97	296	0.44	0.54	5.11	0.23	4.70	0.70	0.75	0.08	-6.89	-36
48	Aspromonte 1	29/05/2000	14.0	7.63	306	194	0.81	0.38	1.10	0.05	1.19	0.80	0.33	n.d.	n.d.	n.d.
49	Aspromonte 2	29/05/2000	14.6	7.39	354	465	3.31	0.64	1.24	0.08	3.40	0.96	0.44	n.d.	n.d.	n.d.
50	Aspromonte 3	02/06/2000	10.2	7.75	387	191	1.38	0.22	0.91	0.05	1.89	0.59	0.31	n.d.	n.d.	n.d.
51	Aspromonte 4	21/03/2000	10.1	6.46	171	149	0.21	0.31	1.05	0.08	0.47	0.75	0.35	n.d.	n.d.	n.d.
52	Aspromonte 5	23/03/2000	13.6	6.68	216	217	0.39	0.49	1.28	0.04	0.81	0.85	0.47	n.d.	n.d.	n.d.
53	Aspromonte 6	18/03/2000	10.8	6.61	120	151	0.22	0.29	0.95	0.05	0.60	0.65	0.36	n.d.	n.d.	n.d.
54	Aspromonte 7	19/03/2000	13.9	7.08	80	215	0.65	0.50	0.86	0.03	1.03	0.59	0.34	n.d.	n.d.	n.d.
55	Sila 1	18/07/1995	12.8	7.46	554	287	0.89	0.38	0.27	0.02	1.34	0.48	0.10	n.d.	n.d.	n.d.
56	Sila 2	18/07/1995	11.7	7.14	514	300	1.20	0.52	0.18	0.02	1.77	0.15	0.10	n.d.	-9.53	-59
57	Sila 3	18/07/1995	13.7	7.64	510	364	1.63	0.56	0.25	0.02	2.21	0.27	0.11	n.d.	n.d.	n.d.
58	Sila 4	12/02/1995	10.1	7.42	285	339	1.72	1.15	0.47	0.03	1.65	0.41	0.48	n.d.	n.d.	n.d.
59	Sila 5	12/02/1995	13.6	7.75	338	326	3.19	0.24	0.27	0.04	3.18	0.21	0.22	n.d.	n.d.	n.d.
60	Sila 6	12/02/1995	13.5	6.29	379	281	1.13	0.48	1.13	0.04	2.13	1.29	0.47	n.d.	n.d.	n.d.

Table 3 – Calculated solute geothermometers for the thermal waters collected over the Calabria Region. The selected thermal waters fall in the field of the partially equilibrated waters (see Figure 5) as defined by Giggenbach (1991). The applied Na/K and Na-K-Ca geothermometers (1, 2, 3) are from Fournier, 1979

Site	Date	Outlet T°C	Quartz	Na/K (1)	Na/K (2)	Na-K-Ca (3)
Antonimine spa	29/06/2000	35.1	67	98	79	72
Antonimine spa	31/10/2001	34.0	70	78	61	92
Caronte spa1	27/06/1994	39.0	86	219	186	139
Caronte spa1	29/10/2001	38.6	41	222	189	144
Cerchiara spa	07/05/1993	27.5	62	180	152	126
Cerchiara spa	28/10/2001	31.8	50	186	157	131
Cerchiara spa	23/01/2007	31.3		185	156	130
Cerenzia spring	14/02/2007	30.7		59	44	28
Cotronei spring	23/06/1994	31.2	57	87	69	43
Cotronei spring	25/06/1994	34.7	59	84	66	55
Cotronei spring	30/10/2001	29.8	46	96	78	74
Cotronei spring	25/01/2007	34.1		85	68	60
Cotronei well	25/06/1994	36.1	67	73	56	30
Cotronei well	30/10/2001	35.2	60	99	80	48
Cotronei well	25/01/2007	35.9		84	67	36
Galatro spa	08/06/1999	37.4	98	119	98	103
Galatro spa	31/10/2001	37.1		95	77	52
Luigiane spa HT	04/02/1995	43.6	86	196	166	162
Luigiane spa HT	13/02/2007	40.0		190	161	155
Luigiane spa LT	13/02/2007	19.7		198	168	145
Nicotera well	26/06/2000	28.2	77	99	80	106
Repole spring	10/02/1995	24.3	43	60	44	62
Repole spring	20/03/2007	24.3		65	49	68
Rosarno well	03/06/2000	26.7	76	50	35	98
S. Calogero well	24/06/2000	29.1	74	110	90	119
Sibarite spa	07/02/1995	23.4	50	241	205	146
Sibarite spa	29/10/2001	25.1		235	200	141
Spezzano spa	07/02/1995	22.8	64	107	88	116
Spezzano spa	29/10/2001	21.8		112	91	117

Table 4- Chemical analyses of the gases dissolved in the thermal waters (4a) and cold waters (4b). Concentrations are expressed in vol%. Starting from the total amount of dissolved gases (cm^3/l at 20°C, see text) we calculated their relative abundances for every single sample and normalized to 100% in volume the analytical results. n.d. = not determined; bdl = below detection limit.

Table 4a

#	Site	Date	He	O_2	N_2	CH_4	CO_2
1	Antonimine spa	31/10/2001	1.72E-01	4.48	94.91	n.d.	0.43
3	Caronte spa1	29/10/2001	1.42E-02	12.72	84.70	0.25	2.32
4	Caronte spa1	27/06/1994	7.93E-02	26.41	70.20	0.01	1.40
4b	Caronte spa2	29/10/2001	5.59E-03	1.20	97.35	0.20	1.24
5	Cerchiara spa	29/10/2001	6.48E-03	n.d.	n.d.	n.d.	n.d.
6	Cerchiara spa	07/05/1993	8.84E-03	15.15	77.05	1.62	3.83
7	Cerchiara spa	23/01/2007	1.06E-02	0.19	94.72	1.27	3.82
8	Cerenzia spring	14/02/2007	1.13E-03	11.59	87.80	0.33	0.28
9	Cotronei spring	30/10/2001	1.12E-01	0.91	98.56	0.42	Bdl
10	Cotronei spring	25/01/2007	1.65E-01	0.13	99.01	0.68	0.01
11	Cotronei spring	23/06/1994	2.92E-01	0.33	95.02	1.71	0.08
12	Cotronei well	30/10/2001	5.86E-02	n.d.	n.d.	n.d.	n.d.
13	Cotronei well	25/01/2007	1.46E-01	0.11	98.79	0.93	0.02
14	Cotronei well	23/06/1994	2.85E-01	0.18	95.45	1.82	0.02
15	Galatro spa	31/10/2001	3.04E-02	1.15	98.47	0.33	0.02
18	Luigiane spa HT	13/02/2007	5.28E-02	0.22	68.98	16.89	13.86
19	Luigiane spa HT	29/06/1994	2.82E-02	29.29	26.54	13.74	29.57
20	Luigiane spa LT	13/02/2007	1.21E-02	0.09	94.40	2.72	2.78
20 b	Luigiane spa LT	08/02/1995	9.83E-02	12.96	75.35	4.50	5.14
22	Palizzi	6/10/2003	6.10E-02	0.01	81.59	18.00	0.03
23	Repole spring	20/03/2007	5.68E-02	0.08	99.66	0.13	0.07
24	Repole spring	10/02/1995	6.93E-02	0.12	96.64	0.01	0.07
27	Sibarite spa well	29/10/2001	5.59E-03	0.95	95.79	0.01	3.25
28	Sibarite spa spring	07/02/1995	3.90E-04	22.45	70.16	1.87	3.29
28b	Sibarite spa spring	29/10/2001	1.38E-03	n.d.	n.d.	n.d.	n.d.
29	Spezzano spa	07/02/1995	6.13E-03	16.15	19.75	63.01	0.31
30	Spezzano spa	29/10/2001	8.40E-04	n.d.	n.d.	n.d.	n.d.

Table 4b

#	Site	Date	He	O_2	N_2	CH_4	CO_2
32	Casabona spring	14/02/2007	5.4E-04	0.03	18.11	1.9E-04	81.86
33	Cassano spring RS	23/01/2007	9.9E-02	0.15	45.96	2.7E-01	53.52
33b	Cassano sulphur spr	23/01/2007	7.2E-05	0.03	10.13	1.8E-01	89.67
34	Cittanova spring	20/03/2007	6.7E-05	4.23	86.79	8.5E-04	8.97
35	Fagnano spring	14/02/2007	6.6E-05	3.98	32.30	1.1E-02	63.71
36	Palmi sulphur spring	20/03/2007	6.2E-05	7.00	91.12	2.1E-03	1.88
37	Polistena spring	20/03/2007	7.7E-05	5.10	83.35	2.1E-04	11.55
38	Rosarno well 1	20/03/2007	9.2E-05	1.35	92.19	2.7E-02	6.43
39	Rosarno well 2	20/03/2007	1.3E-04	0.11	93.87	3.7E-03	6.02
40	Rosarno well 3	20/03/2007	1.3E-04	0.04	89.58	5.7E-02	10.32
41	S. Agata spring	13/02/2007	4.2E-05	0.03	17.85	1.5E-01	81.96
42	S. Ferdinando spr	20/03/2007	5.9E-05	0.06	71.31	7.4E-01	27.88
43	S. Vincenzo spring	23/01/2007	2.7E-04	0.18	34.97	1.6E-02	64.83
44	Strongoli mine spr	23/01/2007	1.0E-02	6.41	40.85	8.8E-04	52.73
46	Verzino sulphur spr	14/02/2007	1.4E-03	0.04	28.50	2.1E-04	71.46
47	Zippone spring	20/03/2007	2.0E-04	0.15	82.85	8.2E-03	16.99

Table 5 – Isotopic composition of carbon: measured $\delta^{13}C_{TDIC}$, and calculated $\delta^{13}C$ of the dissolved CO_2 gas phase and total mass of carbon of both thermal (*Th*) and cold (*C*) springs. Carbon isotope analyses are reported in δ‰ with reference to PDB. Total mass of carbon **is** expressed in mmole per litre

#	Type	Site	Date	$\delta^{13}C_{TDIC}$ ‰ *Measured*	$\delta^{13}C_{CO2}$ ‰ *Calculated*	total carbon *Calculated*
10	*Th*	Cotronei spring	25/01/2007	-6.21	-12.90	1.87
15	*Th*	Galatro Spa	31/10/2001	-6.61	-13.20	1.06
17	*Th*	Laureana di Borrello Well	26/06/2000	-4.58	-12.32	26.77
18	*Th*	Luigiane spa HT	13/02/2007	-2.93	-7.37	14.08
20	*Th*	Luigiane spa LT	13/02/2007	-7.25	-13.00	6.01
23	*Th*	Repole Spring	20/03/2007	-15.56	-23.42	5.59
25	*Th*	Rosarno well	03/06/2000	-3.46	-11.11	19.63
26	*Th*	S.Calogero Well	24/06/2000	-3.67	-10.97	4.41
32	*C*	Casabona spring	14/02/2007	-13.91	-19.84	11.10
33	*C*	Cassano spring RS	25/01/2007	-4.77	-11.98	8.75
34	*C*	Cittanova spring	20/03/2007	-4.79	-12.76	3.12
35	*C*	Fagnano spring	13/02/2007	-10.53	-17.91	7.55
36	*C*	Palmi Sulphur spring	20/03/2007	-2.32	-7.44	3.48
37	*C*	Polistena spring	20/03/2007	-5.53	-12.98	5.03
38	*C*	Rosarno well 1	20/03/2007	-10.45	-19.06	2.74
39	*C*	Rosarno well 2	20/03/2007	-3.81	-12.10	5.48
40	*C*	Rosarno well 3	20/03/2007	-4.22	-12.33	4.77
41	*C*	S. Agata spring	13/02/2007	-13.47	-19.58	13.21
42	*C*	San Ferdinando spring	20/03/2007	-13.55	-21.05	6.31
43	*C*	S. Vincenzo spring	23/01/2007	-9.51	-16.19	6.37
44	*C*	Strongoli mine spr	25/01/2007	-12.55	-16.57	19.12
46	*C*	Verzino spring	14/02/2007	-13.47	-19.91	7.19
47	*C*	Zippone spring	20/03/2007	-3.44	-11.66	5.73

Table 6 – Isotopic analyses of helium dissolved in thermal waters (6a) and cold waters (6b). Air-corrected ratios (R/Rac) are obtained assuming that all the neon in the samples is of atmospheric origin ($^{4}He/^{20}Ne$ ratio of air-saturated water is taken as 0.285).

Table 6a

#	Site	Date	R/Ra	He/Ne	%Atm	%Rad	%Mag	R/Ra c
1	Antonimine spa	31/10/2001	0,06	76,2	0,4	99,6	--	0,05 ± 0,002
3	Caronte spa1	29/10/2001	0,17	10,8	2,9	97,1	--	0,14 ± 0,002
7	Cerchiara spa	30/10/2001	0,06	88,4	0,3	99,7	--	0,05 ± 0,002
8	Cerenzia spring	14/02/2007	0,22	1,0	31,7	68,3	--	0,22 ± 0,003
9	Cotronei spring	30/10/2001	0,10	86,9	0,3	99,7	--	0,10 ± 0,002
10	Cotronei spring	25/01/2007	0,09	97,3	0,3	99,7	--	0,09 ± 0,002
12	Cotronei well	31/10/2001	0,16	17,9	1,8	98,2	--	0,14 ± 0,001
13	Cotronei well	25/01/2007	0,05	116,5	0,2	99,8	--	0,05 ± 0,002
15	Galatro spa	29/10/2001	0,20	6,0	5,3	94,7	--	0,16 ± 0,006
18	Luigiane spa HT	13/02/2007	0,15	3,7	8,5	91,5	--	0,08 ± 0,002
20	Luigiane spa LT	13/02/2007	0,11	21,4	1,5	98,5	--	0,10 ± 0,001
22	Palizzi	06/10/2003	0,17	16,95	1,7	98,3	--	0,16 ± 0,001
23	Repole spring	20/03/2007	0,05	47,1	0,6	99,4	--	0,04 ± 0,001
27	Sibarite well	29/10/2001	0,24	1,3	23,4	76,6	--	0,03 ± 0,005
27b	Sibarite spa	29/10/2001	0,24	4,6	6,9	91,6	1,5	0,19 ± 0,012
29	Spezzano spa	29/10/2001	0,33	1,8	17,9	80,8	1,3	0,20 ± 0,008

Table 6b

#	Site	Date	R/Ra	He/Ne	%Atm	%Rad	%Mag	R/Ra c
32	Casabona spring	14/02/2007	0,29	1,1	27,9	72,1	--	0,05 ± 0,001
33	Cassano spring RS	23/01/2007	0,16	5,0	6,3	93,7	--	0,11 ± 0,003
33b	Cassano spr sulphur	23/01/2007	0,12	18,0	1,7	98,3	--	0,11 ± 0,002
35	Fagnano spring	13/02/2007	0,63	0,4	80,3	19,7	--	0,63 ± 0,018
36	Palmi sulphur spr	20/03/2007	0,88	0,4	82,6	16,5	0,9	0,56 ± 0,011
38	Rosarno well 1	20/03/2007	0,86	0,4	83,9	16,1	--	0,45 ± 0,009
39	Rosarno well 2	20/03/2007	0,58	0,6	54,4	45,6	--	0,19 ± 0,001
40	Rosarno well 3	20/03/2007	0,37	1,0	31,1	68,9	--	0,13 ± 0,004
41	S. Agata spring	13/02/2007	0,61	0,4	77,4	22,6	--	0,61 ± 0,015
43	S. Vincenzo spring	23/01/2007	0,18	1,9	16,1	83,9	--	0,04 ± 0,003
44	Strongoli mine spr	25/01/2007	0,6	0,5	68,6	31,4	--	0,60 ± 0,004
46	Verzino sulphur spr	14/02/2007	0,17	2,5	12,6	87,4	--	0,06 ± 0,001
47	Zippone spring	20/03/2007	0,47	0,6	52,1	47,9	--	0,47 ± 0,001